

**PURDUE UNIVERSITY**  
**GRADUATE SCHOOL**  
**Thesis/Dissertation Acceptance**

This is to certify that the thesis/dissertation prepared

By Elizabeth Ann Osadczuk

Entitled

Characterization of a Cold-Responsive Dehydrin Promoter

For the degree of Master of Science

Is approved by the final examining committee:

Dr. Stephen Randall

Chair

Dr. John Watson

Dr. Christine Picard

To the best of my knowledge and as understood by the student in the *Research Integrity and Copyright Disclaimer (Graduate School Form 20)*, this thesis/dissertation adheres to the provisions of Purdue University's "Policy on Integrity in Research" and the use of copyrighted material.

Approved by Major Professor(s): Dr. Stephen Randall

Approved by: Dr. Simon Atkinson

Head of the Graduate Program

11/14/2013

Date

CHARACTERIZATION OF A COLD-RESPONSIVE DEHYDRIN PROMOTER

A Thesis

Submitted to the Faculty

of

Purdue University

by

Elizabeth A. Osadczuk

In Partial Fulfillment of the

Requirements for the Degree

of

Master of Science

December 2013

Purdue University

Indianapolis, Indiana

I dedicate this to my mom and sister who have helped me through all the stress and were always there for me, even at 3 am. I love you so much.

## ACKNOWLEDGEMENTS

I would like to thank Dr. Randall for all his help; he is always available to help his students both in the lab and classroom. I would also like to thank Dr. Watson for motivating me to be prepared so that I could answer all the questions he was bound to ask at lab meetings. I would also like to thank Dr. Picard for serving on my committee. I likewise would like to thank Dr. Anderson for the use of his fluorescent plate reader. Finally, I would like to thank Yuji Yamasaki and Gage Koehler for their help and patience in all my questions in lab.

## TABLE OF CONTENTS

	Page
LIST OF TABLES .....	vi
LIST OF FIGURES.....	vii
LIST OF ABBREVIATIONS .....	ix
ABSTRACT.....	xi
CHAPTER 1. INTRODUCTION .....	1
1.1 Stress Tolerance .....	2
1.1.1 ABA Dependent Pathways.....	2
1.1.2 ABA Independent Pathways.....	3
1.2 Dehydrins.....	5
1.2.1 Characteristics of Dehydrins.....	6
1.3 Soybeans' Stress Response .....	9
CHAPTER 2. MATERIALS AND METHODS .....	11
2.1 GmERD14prom::GFP/GUS Construct Creation .....	11
2.2 Plant Material and Growth Conditions for <i>Arabidopsis thaliana</i> .....	14
2.3 <i>Agrobacterium tumefaciens</i> Transformation.....	14
2.4 Plant Selection and Line Formation .....	14
2.5 Confirming Genotypes.....	16
2.6 <i>AtERD14</i> prom::ERD14 in ERD14 T-DNA Insertion Lines.....	17
2.7 Tissue Preparation.....	17
2.8 GUS Assay .....	18
2.9 SDS-PAGE and Immunoblotting .....	19
2.10 Protoplast Isolation and Transfection Assays .....	20

	Page
2.10.1	Protoplast Preparation for GUS Assay ..... 21
2.11	RNA Isolation and Analysis ..... 22
CHAPTER 3.	STABLY TRANSFORMED PLANTS' RESPONSE TO COLD STRESS ..... 23
3.1	Results ..... 23
3.1.1	Response of RD29aprom::GFP/GUS to Cold Treatments..... 23
3.1.2	Response of <i>AtERD14</i> prom::GFP/GUS to Cold Treatments ..... 25
3.1.3	Response of <i>AtERD14</i> prom:: <i>AtERD14</i> in ERD14 KO Background to Cold Treatments..... 26
3.1.4	Response of <i>GmERD14</i> prom::GFP/GUS to Cold Treatments ..... 27
3.1.5	Response of <i>AtERD14</i> Transcript to Cold Treatments ..... 27
3.2	Discussion ..... 29
3.2.1	<i>AtERD14</i> , <i>RD29a</i> , and <i>GmERD14</i> Reporter and Protein Response to Cold Treatments..... 29
3.2.2	<i>AtERD14</i> Transcript Has a Slight Response to Cold ..... 32
3.3	Future Plans..... 34
CHAPTER 4.	METHODOLOGY OF PROTOPLAST TRANSFECTION AND GUS ASSAY..... 36
4.1	Results ..... 36
4.1.1	Wavelengths Used to Measure GUS Assay ..... 36
4.1.2	Linear Range of GUS Assay ..... 37
4.1.3	Minimal Amount of Protoplasts ..... 38
4.1.4	Transient Transformation of Protoplasts ..... 38
4.2	Discussion ..... 39
4.3	Future Plans..... 39
REFERENCES	..... 41
TABLES	..... 47
FIGURES	..... 53
APPENDIX	..... 82

## LIST OF TABLES

Table	Page
Table 1: List of all primer sequences used and their targets.....	47
Table 2: Hygromycin resistance of T2 lines used in experiments.....	48
Table 3: Hygromycin resistance of T3 lines used in experiments.....	49
Table 4: Summary of promoter responses to cold treatment.....	51
Table 5: List of attempted cold treatments performed on transformed protoplasts .....	52
Appendix Table	
Table A.1: <i>AtERD14</i> prom:: <i>GFP/GUS</i> GUS reporter is not up-regulated .....	82

## LIST OF FIGURES

Figure	Page
Figure 1: ABA dependent and independent pathways in cold tolerant <i>A. thaliana</i> .....	53
Figure 2: <i>GmERD14</i> prom:: <i>GFP/GUS</i> in pCambia 1304 .....	54
Figure 3: <i>GmERD14</i> and pCambia1304 digest with BamHI and NcoI-HF confirms ligation. ....	55
Figure 4: Sequence of <i>GmERD14</i> promoter following insertion into pCambia1304.....	56
Figure 5: 35S:: <i>GFP/GUS</i> and <i>GmERD14</i> prom:: <i>GFP/GUS</i> stably expressed plant lines contain the insert from transformation. ....	58
Figure 6: <i>RD29a</i> prom:: <i>GFP/GUS</i> and <i>GmERD14</i> prom:: <i>GFP/GUS</i> stably expressed plant lines contain the insert from transformation.....	59
Figure 7: Range of basal level activity in <i>RD29a</i> prom:: <i>GFP/GUS</i> lines.....	60
Figure 8: Analysis of GUS activity from <i>RD29a</i> prom:: <i>GFP/GUS</i> stems.....	61
Figure 9: <i>RD29a</i> prom:: <i>GFP/GUS</i> promoter is cold responsive in T2 stems.....	62
Figure 10: <i>RD29a</i> prom:: <i>GFP/GUS</i> promoter is cold responsive in T3 leaves. ....	63
Figure 11: <i>RD29a</i> prom:: <i>GFP/GUS</i> promoter is cold responsive in seedlings, while <i>GmERD14</i> prom:: <i>GFP/GUS</i> reporter does not increase after cold stress .....	64
Figure 12: Endogenous AtERD14 protein increases in response to cold stress in <i>RD29a</i> prom:: <i>GFP/GUS</i> and <i>GmERD14</i> prom:: <i>GFP/GUS</i> plants.....	65
Figure 13: <i>AtERD14</i> prom:: <i>GFP/GUS</i> is not cold responsive in stems.....	66
Figure 14: <i>AtERD14</i> prom:: <i>GFP/GUS</i> is not cold responsive in seedlings.....	67
Figure 15: <i>AtERD14</i> prom:: <i>GFP/GUS</i> endogenous ERD14 increases in response to cold while GFP reporter shows no similar increase.....	68



Figure	Page
Figure 16: <i>AtERD14</i> prom:: <i>AtERD14</i> expressed in <i>AtERD14</i> KO increases in response to cold.....	69
Figure 17: <i>GmERD14</i> prom:: <i>GFP/GUS</i> is not cold responsive in T3 leaves.....	70
Figure 18: <i>AtERD14</i> transcript is slightly up-regulated under cold stress when not normalized to <i>AtEF1<math>\alpha</math></i> .....	71
Figure 19: <i>AtEF1<math>\alpha</math></i> reference gene transcript is upregulated under cold stress .....	72
Figure 20: <i>RD29a</i> transcript is strongly up-regulated under cold stress .....	73
Figure 21: Optimal emission wavelength for detection of MU in the presence of the lysis buffer and MUG is 460nm .....	74
Figure 22: Optimal excitation wavelength for detection of MU in the presence of the lysis buffer and MUG is 360nm .....	75
Figure 23: Linearity of GUS Assay, fluorescence as a function of MU concentration.....	76
Figure 24: Saturation point of GUS Assay .....	77
Figure 25: Linearity of GUS Assay as a function of GUS concentration .....	78
Figure 26: Protoplasts were successfully transiently transformed .....	79
Figure 27: <i>RD29a</i> prom:: <i>GFP/GUS</i> was successfully transformed into <i>Arabidopsis thaliana</i> protoplasts.....	80
Figure 28: <i>35S</i> :: <i>GFP/GUS</i> is successfully transformed into protoplast cells.....	81
Appendix Figure	
Figure A.1: <i>GmERD14</i> prom:: <i>GFP/GUS</i> promoter is not cold responsive in T2 stems.....	83

## LIST OF ABBREVIATIONS

ABA	abscisic acid
ABF	abscisic response factor
ABI/PP2C	abscisic acid insensitive 1/type C2 protein phosphatase
ABRE	abscisic acid responsive element
AREB	abscisic acid responsive element binding protein
At	<i>Arabidopsis thaliana</i>
bp	base pair
CAMTA	calmodulin-binding transcription factor
CBF	C-repeat/dehydration responsive element binding factor
cDNA	complementary DNA
CRT	C-repeat
DRE	dehydration response element
DBEB	dehydration responsive element-binding protein
ERD	early response to dehydration
GFP	green fluorescent protein
Gm	Glycine max (soybean)
GUS	$\beta$ -glucuronidase

HF	high fidelity
HOS	high expression of osmotically responsive gene
HSP	heat shock protein
ICE	inducer of CBF expression
kb	kilobases
LEA	late embryogenesis abundant
min	minute
MU	4-methylumbelliferone
MUG	4-methylumbelliferyl- $\beta$ -D-glucuronide
PCR	polymerase chain reaction
PYR1/PYL/RCAR	pyrabactin resistance 1/pyr-like/regulatory component of ABA receptor
RAB	responsive to abscisic acid
RD	response to dehydration
RFU	real fluorescent unit
ROS	reactive oxygen species
RuBisCO	ribulose-1, 5-bisphosphate carboxylase/oxygenase
SIZ	small ubiquitin-like modifier (SUMO) E3 ligase
SnRK2 kinase	sucrose non-fermenting 1-related protein kinase 2
SUMO	small ubiquitin-related modifier
UTR	untranslated region

## ABSTRACT

Osadczuk, Elizabeth A. M.S., Purdue University, December 2013. Characterization of a cold-responsive dehydrin promoter. Major Professor: Stephen K. Randall.

Dehydrins are type II LEA proteins induced in many plants during drought, low temperature, and high salinity to confer stress tolerance. *AtERD14* is an *Arabidopsis thaliana* dehydrin that functions in part of the cold stress pathway. *AtERD14* has chaperone-like capabilities that allow it to bind and protect various proteins from dehydration stresses. In order to determine the necessary components for cold induction of *AtERD14*, *AtERD14*prom::*GFP/GUS* and *AtERD14*prom::*AtERD14* in *AtERD14* KO constructs were created and stably transformed into *A. thaliana*. Analysis of the constructs showed the *AtERD14* promoter alone was insufficient to respond to cold, and it was necessary to attach the *AtERD14* coding region to the promoter to induce a cold response in ERD14. On the other hand, the *RD29a*prom::*GFP/GUS* promoter did respond to cold stress, indicating that *RD29a* does not require its coding region to support an increased amount of reporter activity after cold stress. The protoplast transformation system, while capable of transient expression of introduced constructs in protoplasts, was difficult for use for cold-inducible expression.

## CHAPTER 1. INTRODUCTION

The world population has already reached 7 billion and is expected to exceed 9 billion people by 2050 (Smith, 2010). Currently, 842 million people world-wide, or one-eighth of the population, live without enough food (FAO, 2013). Lack of proper nutrition causes 45% of deaths in children under the age of five each year (which is 3.1 million deaths yearly) (Black, 2013). In a world where food shortages are already a problem, one of the dilemmas of our world will be how to feed our growing population. Abiotic stress, including drought, high salt, and cold temperatures is the primary cause of decreased crop yield and causes over 50% of most major crop loss worldwide (Qin, 2011). Because plants are unable to avoid their stressors, they must adapt and acquire ways to cope with their surrounding environment and these stresses. By better understanding how plants respond to abiotic stress, we can hope to create hardier crops. This is especially important when dealing with crops that are less stress tolerant, like soybean

## 1.1 Stress Tolerance

Osmotic stress is a common component of drought, high salt, and cold stress (Chinnusamy, 2004). As a result, abiotic stress responses utilize common pathways. The abscisic acid (*ABA*) dependent and independent pathways are two such important pathways in osmotic response. In a cold tolerant plant such as *Arabidopsis thaliana*, the *ABA* dependent and independent pathways activate many stress tolerance genes, including dehydrins.

### 1.1.1 ABA Dependent Pathways

Osmotic stress, and especially drought and high salinity stress, causes an increase in *ABA* levels (Qin, 2011). Under stress-free conditions, the negative regulator ABA Insensitive 1/ Type C2 Protein Phosphatase (*ABI/PP2Cs*) dephosphorylates Sucrose Non-Fermenting 1-Related Protein Kinase 2 (*SnRK2* kinases). The dephosphorylated *SnRK2* is inactive and prevents the *ABA* signal. When *ABA* is present, the *ABA* receptor Pyrabactin Resistance 1/Pyr-Likes/Regulatory Component of ABA Receptors (*PYR1/PYLs/RCARs*) binds to both *ABA* and *ABI/PP2Cs*. Once the receptor binds to *ABA* it deactivates the *ABI/PP2Cs*, preventing the dephosphorylation of *SnRK2*. With the negative regulator *ABI/PP2Cs* activity inhibited, *SnRK2* becomes phosphorylated and in turn activates bZIP transcription factors. Some examples of bZIP transcription factors include ABA-Responsive Element-Binding protein/ABA Responsive Factor (*AREBs/ABFs*).

*AREBs/ABFs* then bind to *ABA* responsive elements (ABRE) sequences located in the promoters of stress responsive genes, including dehydrins, to increase the gene expression (Figure 1) (Qin, 2011).

### 1.1.2 ABA Independent Pathways

C-repeat-binding factor/dehydration responsive element-binding protein (CBF/DREB) transcription factors are unique to plant species and are the key players of several *ABA* independent signaling pathways. In *ABA*-independent responses to drought and high salinity stress, *DREB2A* is a key transcription factor (Ciarmiello, 2011). *DREB2A*-interacting protein 1 and 2 (*DRIP1* and *DRIP2*) ubiquitin E3 ligases are negative regulators of *DREB2A*. Under normal conditions, *DRIP1/2* will cause ubiquitination of *DREB2A* (Qin, 2008). During ubiquitination, four ubiquitin are added to the *DREB2A*. The ubiquitin then signals *DREB2* to be targeted to the 26S proteasome where it will be degraded. Under drought and heat stress, *DREB2A* is not degraded and will bind to dehydration responsive elements (DRE) sequences in the promoters of various stress responsive genes to up-regulate their expression levels (Figure 1) (Chinnusamy, 2004).

While exogenous treatment of *ABA* will induce many cold responsive genes, *ABA* independent pathways are the primary controller of cold inducible genes (Shinozaki, 2000). The transcription factor *CBF/DREB1* is the major regulator of *ABA* independent cold stress response in plants (Chinnusamy, 2004; Ciarmiello, 2011; Qin, 2011). Two regulating elements of *CBF* are Myc and CM2 cis-elements found in the *CBF* promoter (Qin, 2011). *ICE1* (inducer of *CBF* expression) is a transcription factor that binds to the

Myc sequence (Chinnusamy, 2004) to activate *CBF*. *ICE1* is constitutively expressed in cold tolerant plants and must be activated in order to bind to *CBF* (Qin, 2011). Calmodulin-binding transcription factor 3 (*CAMTA3*) binds to CM2 and also acts as an activator of the gene to promote *CBF* expression (Figure 1) (Qin, 2011).

*ICE1* is modified by both high expression of osmotically responsive gene 1 (*HOS1*) and SAP and Miz1 (*SIZ1*) to regulate its quantity and activation in response to a cold stress. *HOS1* is a negative regulator of *CBF* genes while *SIZ1* is a positive regulator. Both *HOS1* and *SIZ1* are activated by cold stress to cause a fast, transient *CBF* up-regulation in response to cold stress (Thomashow, 2010; Qin, 2011). Early on in the cold stress, *SIZ1*, a small ubiquitin-related modifier (*SUMO*) E3 ligase targets the K393R residue in *ICE1* to undergo sumoylation. The sumoylation activates the *ICE1* protein, which allows it to bind to Myc and activate *CBF* (Qin, 2011). *HOS1* acts in opposition to *SIZ1*. *HOS1* is an E3 ligase that ubiquitinates *ICE1* to prevent it from binding to and activating *CBF*. *HOS1* is expressed in the cytoplasm when there is no stress, but following a cold signal it is translocated into the nucleus. Once in the nucleus, it is able to interact with and ubiquitinate *ICE1* (Thomashow, 2010). The time delay while *HOS1* is translocated gives *SIZ1* time to up-regulate *ICE* (and thereby activate *CBF*). However, once *HOS1* is in the nucleus, *ICE1* activity is again decreased, causing a transient cold response (Qin, 2011). It has also been suggested that the sumoylation of *ICE1* may act to prevent ubiquitination of *ICE1* and thus counter-act *HOS1* activity to an even greater degree (Miura, 2007).



After *CBF* is activated, it binds to C-repeat (CRT) or dehydration responsive elements (DRE) (A/GCCGACNT) sequences in the promoters of dehydrins and other stress responsive genes (McKhann, 2008) in order to activate these genes. Dehydrins that are strongly induced by cold stress may contain many CRT/DRE elements in their promoters (Chinnusamy, 2004). However, they often contain ABRE elements (ACGTGG/TC) (Narusaka, 2003), which allow these genes to respond to both the *ABA* dependent and *ABA* independent pathways. On the other hand, a gene that is mainly activated by drought may contain many ABRE elements, and only one or two CRT/DRE elements. Thus both the *ABA* dependent and independent pathways are interconnected and able to activate many of the same genes.

## 1.2 Dehydrins

Drought, high salinity, and cold stress all lead to the loss of intracellular water, or cell dehydration (Hanin, 2011). The most frequent mechanism developed by plants to combat water stress is accumulation of late embryogenesis abundant (LEA) proteins (Hanin, 2011) in the *ABA* dependent and independent pathways.

LEA proteins are named because they are abundant during late stages of embryogenesis (Close, 1997), where they may represent as much as 4% of cellular proteins within the plant (Hanin, 2011). Dehydrins are a distinct family of LEA proteins, the group 2 LEA (or LEA II) proteins that accumulate not only in the later stages of embryo development but also in vegetative tissues in response to abiotic stresses that lead to cell dehydration (Close, 1997). Because several dehydrins accumulate in

response to *ABA* (via the *ABA*-dependent pathway), these proteins are also known as responsive to *ABA* (RAB) proteins (Hanin, 2011).

Dehydrins are used as a marker for a plant's capability to withstand abiotic stressors. In several plants, including *A. thaliana* (Puhakainen, 2004), *Fragaria spp.* (strawberry) (Davik, 2013), and *Gramineae* (wheat) (Houde, 1992), there is a direct correlation between the amount of dehydrins accumulated in response to an abiotic stress and the level of plant tolerance towards the stress. This relationship was clearly seen when Puhakainen (2004) created *A. thaliana* lines overexpressing both an acidic and a basic dehydrin. These lines were exposed to a -10°C freezing stress and had a significant increase in survivorship (75-86%) compared to wildtype *A. thaliana* survivorship (18-22%).

### 1.2.1 Characteristics of Dehydrins

Dehydrins are defined as proteins containing at least one copy of the lysine-rich K segment [EKKGIM(E/D)KIK(I/E)KLPG] near their C terminus (Nylander, 2001; Hanin, 2011). The K segment is highly conserved in higher and lower plants (Close, 1997) and can appear in 1 to 11 copies within a single dehydrin (Hanin, 2011). Dehydrins may also contain Y segments, S segments, and  $\phi$  segments (Close, 1997). The Y segment [(V/T)D(E/Q)YGNP] is a tyrosine containing segment near the N-terminus of the dehydrin (Hanin, 2011). The S segment is a serine rich segment containing four to 10 consecutive serines (LHRSGS4-10(E/D)3) (Hanin, 2011). The  $\phi$  segments are less conserved but high in glycine and polar amino acids. When present,  $\phi$  segments of

dehydrins are usually tandemly repeated between K segments (Close, 1997). Dehydrins are placed into one of five structural subgroups, Kn, SKn, KnS, YnKn, and YnSKn, based on the presence or absence, number, and order of K, Y, and S segments within a dehydrin (Hanin, 2011).

The serines on the S segment can undergo phosphorylation (Alsheikh, 2003; Alsheikh, 2005) and can be responsible for translocation of the dehydrin from the cytoplasm to the nucleus (Hanin, 2011). However, phosphorylation is not a requisite as there have been dehydrins located in the nucleus that lack S segments (Hanin, 2011). In other dehydrins, such as *A. thaliana* early response to dehydration 14 (*AtERD14*), phosphorylation activates the protein to bind cations (Alsheikh, 2003).

The K segment is mandatory for a dehydrin as it is thought to be responsible for the shape changes that dehydrins undergo to provide their protective function. When placed in an aqueous solution, dehydrins appear to be largely unstructured and form a random coil (Hanin, 2011). However under cell dehydration, dehydrins' conformation changes as the K segments assume an amphipathic  $\alpha$ -helical conformation (Hanin, 2011). In this conformation, the K segments can bind with the surfaces of partially dehydrated proteins, biomembrane surfaces, and other K segments located in the same dehydrin that are also in the  $\alpha$ -helix formation. When K segments bind to other proteins or membranes, they are thought to provide stability to the structure, thus preventing further damage (Koag, 2003). Without this protection, dehydration would change the protein's conformation and cause it to denature. Dehydrins are therefore thought to be

able to act partially as chaperones do, helping other proteins to fold properly and preventing them from aggregating during dehydration stress. (Hanin, 2011).

AtERD10 and AtERD14 dehydrins both exhibit this chaperone-like activity and are able to protect protein substrates from aggregating/deactivation under heat stress (Kovacs, 2008). These dehydrins appear relatively nonspecific in their binding, allowing them to provide a wide range of protection (Kovacs, 2008). Furthermore, the protective abilities of ERD14 and ERD10 in some instances rivaled or even surpassed the protective capability of HSP90, a chaperone found in eukaryotes (Kovacs, 2008).

When multiple K segments bind together, this increases the amphipathic ability of the  $\alpha$ -helix, thus increasing their ability to form interactions with proteins and membranes (Hanin, 2011). Likewise, once a dehydrin is bound to other proteins, it increases its amphipathic  $\alpha$ -helical conformation, allowing it to protect additional proteins (Hanin, 2011).

A final protective property is the ability of dehydrins to act as an antioxidant. Dehydrins have been found to act as reactive oxygen species (*ROS*) scavengers (Hara, 2004) and bind to metal ions (Hara, 2005; Hanin, 2011). Under stress, plants produce an increased number of *ROS* (O'Brien, 2012). *ROS* are chemically active molecules that can cause a decrease in photosynthesis, increase electrolyte leakage, and increase apoptosis (or cell death) (O'Brien, 2012). As a *ROS* scavenger, dehydrins will remove *ROS* to prevent the harmful built-up (Hara, 2004). The citrus dehydrin *CuCOR15* was found to bind to  $\text{Fe}^{+3}$ ,  $\text{Co}^{+2}$ ,  $\text{Ni}^{+2}$ ,  $\text{Cu}^{+2}$ , and  $\text{Zn}^{+2}$  (Hara, 2005). *CuCOR15* exhibited the highest affinity for copper ions, and was able to bind to 16  $\text{Cu}^{+2}$  at once (Hara, 2005). By binding

metal ions, dehydrins prevents the synthesis of new *ROS*, thus using another mechanism to prevent the build-up of *ROS* within a stressed plant (Hara, 2005; Rorat, 2006; Hanin, 2011).

### 1.3 Soybeans' Stress Response

Different plants recognize and respond to stress in different ways. As a result, plants exhibit different levels of tolerance to stress (Chinnusamy, 2004). The model plant *A. thaliana* is a cold tolerant plant and is able to survive temperatures at  $-10^{\circ}\text{C}$  after a previous cold exposure at  $4^{\circ}\text{C}$  (Gilmour, 1988). Soybean (*Glycine max*) is a cold sensitive plant and is not able to acclimate to a cold stress (Chinnusamy, 2007). As it stands, farmers must choose between planting their soybeans earlier to produce greater yield versus the risk of an unexpected frost damaging the crop. Because of soybean's wide-spread use for food, animal feed, and oil, it is important to study the abiotic stress response of soybean in order to understand what makes it so susceptible to cold stress.

In *A. thaliana*, both *CBF* and the *CBF*-regulated dehydrin genes are up-regulated in response to cold stress. Specifically, the dehydrin *ERD14* (early response to dehydration 14), has been shown to respond to cold stress in *A. thaliana* (Kiyosue, 1994). The *AtERD14* promoter contains both ABRE and CRT/DRE elements, meaning it can respond to both the ABA-dependent and independent pathways. Our lab has previously identified *CBF* and *ERD14* homologues in soybean (*GmCBF* and *GmERD14*) and noted that while *GmCBF* 1 and 2 transcription levels are upregulated under cold stress (Yamasaki and Randall, unpublished data), the corresponding *GmERD14* is not

upregulated after cold stress (Yamasaki, 2013). Therefore, it is plausible that one reason soybeans are cold intolerant is that they have a defect in the cold response pathway somewhere after *CBF* transcription yet before dehydrin transcription (Figure 1). My initial hypothesis was that soybeans are cold intolerant because their dehydrin promoters are not cold responsive and are unable to properly regulate transcription of their associated genes.

To determine whether the *GmERD14* promoter has the capability to respond to cold signals, I analyzed the functionality of the *GmERD14* promoter in *A. thaliana*. The *GmERD14* promoter was inserted into a plasmid (pCambia 1304) containing a GFP/GUS reporter. Because *A. thaliana* is cold tolerant, we know the cold-responsive machinery is present and functional. Therefore, if the *GmERD14* promoter driving a reporter gene does not respond to cold stress, it would indicate that soybeans' dehydrin promoters cannot respond appropriately to cold stress. Both *AtERD14* and *A. thaliana* response to dehydration 29a (*AtRD29a*) promoter and reporter constructs were transformed into *A. thaliana* as positive controls. The *RD29a* promoter contains several CRTs and one ABRE, so it is activated primarily through the ABA independent pathway and is strongly cold induced (Msanne, 2011).

## CHAPTER 2. MATERIALS AND METHODS

### 2.1 GmERD14prom::GFP/GUS Construct Creation

A construct of *GmERD14* promoter was introduced into pCambia 1304 (Figure 2) and used to stably transform *A. thaliana*. Soybean DNA extraction was performed on soybean cultivar Young using the Invitrogen plant DNAzol® reagent protocol provided by the manufacturer (Life Technologies). PfuUltra Fusion II® polymerase (Pfu PCR) (Agilent) was used to amplify genomic soybean DNA using primers specific to *GmERD14* (*GmERD14* forward and *GmERD14* reverse primers) (Table 1). Thermal cycling was performed with a Perkin Elmer GeneAmp PCR System 2400 using an initial cycle of two minutes at 95°C, followed by 35 cycles of one minute at 95°C, 1 minute at 58°C, and two minutes at 68°C, with a final extension of five minutes at 68°C. The amplified product length was expected to be around 3800 bp. The PCR product was loaded onto a 1% agarose gel, the appropriate band was excised and purified using a QIAquick® Gel Extraction Kit (Qiagen). The PCR band was cloned into Zero Blunt (using Zero Blunt® PCR cloning kit from Invitrogen) and then transformed into Top10 competent cells (Invitrogen) and colonies were grown overnight. Plasmid mini-prep of individual colonies was performed, and an EcoRI digestion was performed to identify possible

clones containing *GmERD14*. Pfu PCR using primers containing the restriction enzyme sites BamHI and NcoI was performed on plasmid DNA (*GmERD14* BamHI forward and *GmERD14* NcoI reverse primers) (Table 1). Cycling was done at 95°C for three minutes, 54°C for one minute, 68°C for two minutes, 95°C for one minute, 54°C for one minute, 68°C for two minutes (these cycle steps were performed to integrate the NcoI and BamHI restriction sites from the primer ends into the ends of the *GmERD14* promoter sequence), followed by 20 cycles of 95°C for one minute, 63°C for one minute, and 68°C for two minutes, and a final extension of 68°C for five minutes. The expected product size was 2160 bp. PCR products were separated on a 1% agarose gel; the 2160 bp band was extracted and purified using a QIAquick® kit (Qiagen). The purified band was cloned into Zero Blunt and transformed into Top10 cells (Invitrogen). Top10 colonies were grown overnight and plasmid mini-preps were completed over several individual colonies. Next, 5 µg of the plasmid DNA containing *GmERD14* was digested with restriction enzymes BamHI and NcoI-HF using NEBuffer4 with BSA (NEB). At the same time, 5 µg of the plasmid vector pCambia1304 was also digested with BamHI and NcoI-HF. DNA was then separated on a 1% agarose gel. For *GmERD14*, five expected bands appeared (2160, 1577, 1463, 438, and 40 bp). The uppermost band (2160 bp) contained the *GmERD14* promoter region. For the pCambia1304 samples, two expected bands appeared (11,569 and 792 bp). The upper pCambia1304 band contained the reporter gene (GFP/GUS) and resistance markers (Kanamycin and Hygromycin B). The lower pCambia1304 band contained the 35S promoter (which is being replaced with the *GmERD14* promoter). The appropriate products of both samples (2160 and 11,569 bp)



were extracted by cutting the bands out of the gels and purified using a QIAquick® kit (Qiagen). Overnight ligation of pCambia1304 and *GmERD14* promoter was performed using a 1:3 vector to insert ratio. The ligated product was then transformed into top10 cells and colonies were grown overnight. A mini-plasmid prep was performed on individual colonies. To confirm the ligation, a digest using Bam HI and NcoI-HF was performed. A 1% agarose gel was run and the expected 2160 (*GmERD14* promoter insert) and 11,569 (pCambia1304 vector) bp bands appeared (Figure 3). The sample was then sequenced by the DNA Sequencing Core Facility at IUPUI using GFP reverse, *GmERD14* sequencing forward, *GmERD14* sequencing reverse1, and *GmERD14* sequencing reverse2 primers. A 100% match of the *GmERD14* promoter segment was obtained except for an extra nucleotide N located in the BamHI site between the predicted G and A nucleotides (Figure 4). However, when viewing the chromatograph, A appeared as a prominent peak after the G in the sequence. Compression caused by a series of three C nucleotides followed by four G nucleotides caused a space between the final G and following A nucleotide, which the computer read as an extra N (Figure 4). BamHI restriction enzyme also digested at this point, indicating the proper sequence was a complete match in this area. All steps involving kits were completed by following the protocols provided by the manufacturer. The *RD29aprom::GFP/GUS*, *AtERD14prom::GFP/GUS*, and *AtERD14prom::AtERD14* constructs used in this study were generated similarly (Yamasaki and Randall, unpublished).

## 2.2 Plant Material and Growth Conditions for *Arabidopsis thaliana*

*Arabidopsis thaliana* ecotype Columbia II (C907) seeds were placed on the surface of moistened soil (PRO-MIX), covered with a plastic cover, and placed at 4°C for four days stratification in the dark. Plants were then moved to 20°C. Plants were watered and fertilized regularly and were grown in a plant growth chamber with 18h light/6h dark. Cold treatments lasted for 24 hours at 4°C in the same light conditions. Samples were collected before and after cold treatment at four hours after dawn. Two-month-old stems or one month old leaves were harvested and frozen in liquid nitrogen and stored in a -80°C freezer.

## 2.3 *Agrobacterium tumefaciens* Transformation

GV3101 *Agrobacterium* chemically competent cells were used in all transformations (TAIR: <http://www.arabidopsis.org/>) following Zhang (2006) protocol. *RD29a*prom::*GFP/GUS*, *GmERD14*prom::*GFP/GUS*, or 35S::*GFP/GUS* in pCambia1304 was transformed into *A. thaliana*. A modified floral dip method was used where the *Agrobacterium* solution was pipetted onto unopened rosettes (Martinez-Trujillo, 2004). Plants were matured, dried out, and seeds were collected.

## 2.4 Plant Selection and Line Formation

Hemizygous *RD29a*prom::*GFP/GUS*, *GmERD14*prom::*GFP/GUS*, or 35S::*GFP/GUS* seed populations were grown on selection plates with 1/2X Murashige and Skoog with macro- and micro-nutrients (MS) as described by Murashige and Skoog (1962)

containing 0.05% MES, pH 5.7, and 0.8% bactoagar. After autoclaving and cooling, a final concentration of 15  $\mu\text{g}/\text{mL}$  Hygromycin B was added and 30 mL was poured per plate (Harrison, 2006).

Seeds were sterilized by covering them in 95% ethanol for 5 min, 20% Clorox® bleach (sodium hypochlorite) for 20 min, and then washed five times with autoclaved water. Seeds were then placed on the 1/2X MS plates. Plates were then placed in the dark at least two days at 4°C and then transferred to a growth chamber in the light for six hours at 22°C. They were then placed in the dark for two days at 22°C. Finally, they were placed in the light for one day at 22°C (Harrison, 2006). After this time period, seeds that contained the hygromycin resistance were counted and selected to be transferred to soil. Seeds that contained the resistance marker have long hypocotyls versus the short hypocotyls of hygromycin sensitive plants.

After transplanting the hemizygous (T1) seeds onto soil, these plants were allowed to flower inside sleeves. Each T1 seed represented a separate transformation event and was therefore a separate line. Sleeves prevent cross-pollination and ensured flowers were self-fertilized. Seeds were harvested and T2 seed populations were planted on hygromycin plates. If there was a single insertion event, T2 seed populations were expected to contain 1:2:1 ratio of homozygous:heterozygous:wildtype seeds. T2 seeds were evaluated for hygromycin resistance as describe above (Harrison, 2006). Results are shown in Table 2. Next, seeds that contained the hygromycin resistance were transplanted to soil and forced to self-pollinate. Seeds were collected from the T2 parents and these seeds are T3 individuals. T3 seeds were planted on hygromycin plates

and the number of resistance seeds was counted to determine which population came from T2 homozygous individuals and therefore are homozygous populations (Table 3). *RD29aprom::GFP/GUS* expressing seedlings were slightly dwarfed, making it difficult to properly evaluate their resistance by the long hypocotyl test (hygromycin B). The *AtERD14prom::GFP/GUS* and *AtERD14prom::AtERD14* homozygous lines were similarly obtained (Yamasaki and Randall lab, unpublished).

## 2.5 Confirming Genotypes

DNA extraction was performed using the Invitrogen plant DNAzol® reagent protocol provided by the manufacturer (Life Technologies). A slight modification was made as all plant material and reagent values were reduced by half. To confirm the presence of plasmid inserts, PCR was run using GoTaq® polymerase (Promega) using primers specific to the plasmid insert after *Agrobacterium* transformation. The *RD29aprom::GFP/GUS* segment was amplified using *Rd29a* BamHI forward and GUS reverse primers (Table 1) with an initial 2 minutes at 94°C, followed by 30 cycles of 94°C for 30 seconds, 59°C for 45 seconds, and 72°C for 3 minutes, and a final extension at 72°C for 5 minutes. The *GmERD14prom::GFP/GUS* segment was amplified using the GUS forward and the GUS reverse primers (Table 1) with an initial 2 minutes at 94°C, followed by 30 cycles of 94°C for 30 seconds, 57°C for 45 seconds, and 72°C for 1 minute, and a final extension at 72°C for 5 minutes. The *35S::GFP/GUS* (empty vector) segment was amplified using the 35S forward and the GUS reverse primers (Table 1) with an initial 2 minutes at 94°C, followed by 30 cycles of 94°C for 30 seconds, 56°C for 45

seconds, and 72°C for 1 minute and 12 seconds, and a final extension at 72°C for 5 minutes. Expected PCR products were 3618 bp for the RD29aprom::*GFP/GUS*, 965 bp for the *GmERD14*prom::*GFP/GUS*, and 2220 bp for the 35S::*GFP/GUS* (Figure 5 and 6).

## 2.6 *AtERD14*prom::*ERD14* in *ERD14* T-DNA Insertion Lines

*AtERD14* knock-out (KO) lines were obtained using SM\_3\_40483 T-DNA insertion mutation (TAIR: <http://www.arabidopsis.org/>) in the At1g76180 gene corresponding to *AtERD14*. The insertion was verified and the pCambia1304 plasmid containing *AtERD14*prom::*ERD14* was transformed into *AtERD14* KO (Yamasaki and Randall lab, unpublished). A transformation containing the pCambia1304 plasmid (35S::*GFP/GUS*) was also inserted into the *AtERD14* KO (Yamasaki and Randall, unpublished). The *AtERD14*prom::*GFP/GUS* and *AtERD14*prom::*AtERD14* sequences both contain the same *AtERD14* promoter sequence. This *AtERD14* promoter sequence is the 2,572 base pairs immediately in front of the *AtERD14* ATG start codon (and therefore also contains the 5' UTR). The *AtERD14* coding sequence was isolated from cDNA and does not contain either the 3' UTR or the single 87 bp intron in the middle of the *AtERD14* coding region.

## 2.7 Tissue Preparation

Cold treatments were performed on seedlings grown on 1/2X MS plates. Plates were placed in a black box for four days at 4°C. Plates were then transferred to a growth chamber with 18h light/6h dark at 20°C. Seedlings were grown for two weeks starting from the time the plates were transferred to the light. Whole seedlings were

removed from plates and frozen in liquid nitrogen. All healthy seedlings from a plate (at least 20 per plate) were collected in liquid nitrogen as one sample. Seedlings were collected before and after 24 hour cold treatments at 4°C.

Tissue samples (seedlings, leaves, and stems) were pulverized to a fine powder using liquid nitrogen to prevent thawing. Leaves (0.1 g), stems (0.1 g) and whole seedlings (0.05-0.1g) were placed in 250  $\mu$ L of modified lysis buffer containing 2.5mM Tris-phosphate (pH 7.8) with 1 mM DTT, 2 mM EDTA, 10% (v/v) glycerol, and 0.1% (v/v) Triton X-100 (Yoo, 2007). Samples were homogenized and spun down at 17000 g for 10 minutes. The supernatant was transferred to a new tube and the pellet was discarded. An aliquot was removed for protein concentration quantification via a Bradford assay (Bradford, 1976) and the remainder was frozen at -80°C. When samples were thawed for further analysis, they were all diluted to the same concentration within a sample set (0.5 to 1  $\mu$ g/ $\mu$ L).

## 2.8 GUS Assay

Tissue samples that contained the GFP/GUS reporter were analyzed using a GUS assay to compare basal and cold induced GUS levels. Ten  $\mu$ L of the sample in lysis buffer and 100  $\mu$ L of modified MUG substrate mix containing 10 mM Tris-HCl (pH 8), 1 mM MUG dissolved in the smallest possible volume of DMSO (150  $\mu$ L of DMSO used to dissolve 0.0264 g MUG, 500 mM), and 2 mM MgCL<sub>2</sub> (Yoo, 2007). Fluorescence was measured

continuously for 60 to 90 minutes at 37°C on a Spectramax M2® (Molecular Devices) in a 96 well format (Fior, 2009). Excitation was set for 360 nm and emission was set at 460 nm.

## 2.9 SDS-PAGE and Immunoblotting

Unless indicated otherwise, proteins were separated by 10% SDS-PAGE (Laemmli, 1970). For immunoblotting, the gel was equilibrated in Western transfer buffer (25 mM Tris, 192 mM glycine, and 20% (v/v) methanol) for 30 minutes. Gels were then transferred to PROTRAN® BA85 nitrocellulose membrane with 0.45 µm pore size. Transfers occurred overnight at 0.2 Amps at 4°C. The nitrocellulose gel was soaked in 1XPBS/5% milk (137 mM NaCl, 2.7 mM KCl, 4.3 mM Na<sub>2</sub>HPO<sub>4</sub>, 1.47 mM KH<sub>2</sub>PO<sub>4</sub>/5% Nestle® Carnation instant nonfat dry milk pH to 7.4) for three hours to block non-specific binding sites. Primary antibody was incubated for three hours at room temperature or overnight at 4°C in 1XPBS/5% milk. Nitrocellulose membranes were then washed three times in 1XPBS/5% milk for 15 minutes each. The secondary antibody::horseradish peroxidase conjugate was incubated in 1XPBS/5% milk for 45 minutes at room temperature. The membrane was then washed three times in 1XPBS/5% milk for 15 minutes each and additionally washed twice in 1XPBS for 20 minutes each. Imaging was done using SuperSignal® West Dura Extended Duration Substrate (Thermo Scientific) to detect the secondary antibody. To detect the ERD14 protein, the primary antibody anti-ERD14 (Nylander, 2001) was used in a 1:10,000 ratio followed by the secondary antibody anti-rabbit:peroxidase in a 1:2000 ratio. To detect GFP, the primary

antibody anti-GFP (abcam® ab290-50) was used in a 1:5000 ratio followed by the secondary antibody anti-rabbit:peroxidase in a 1:2000 ratio. A separate 10% SDS-PAGE was run and the ribulose-1,5-bisphosphate carboxylase oxygenase (RuBisCO) protein (coomassie-stained) was used as a loading control.

### 2.10 Protoplast Isolation and Transfection Assays

A combination of Wu (2009) and Yoo (2007) protocols were used for protoplast transformation assays. A 'Tape-*Arabidopsis* Sandwich' was created by placing Fisherbrand tape (similar to Time tape) on the upper epidermal layer of the *A. thaliana* leaf and Scotch tape on the lower epidermal layer of the *A. thaliana* leaf. The Scotch tape was peeled off to remove the lower epidermal layer. Ten to 15 exposed leaves were then placed face down in a Petri dish containing 10 mL enzyme solution (1% (w/v) cellulose R10, 0.25% (w/v) macerozyme R10, 0.4 M mannitol, 10 mM CaCl<sub>2</sub>, 20 mM KCl, 0.1% BSA, and 20 mM MES pH 5.7). The Petri dish was shaken at 40 rpm in the light for 60 minutes. The protoplasts were centrifuged at 100g for three minutes in a Beckman GS-6R Centrifuge. The supernatant was removed and the protoplast pellet was re-suspended by gentle swirling. The protoplasts were washed twice with 25 mL W5 solution (154 mM NaCl, 125 mM CaCl<sub>2</sub>, 5 mM KCl, 5 mM glucose, and 2 mM MES pH 5.7) and placed on ice for 30 minutes in W5 solution. Experiments where protoplasts were later subjected to cold treatments were kept at room temperature. During the 30 minute incubation period, protoplasts were counted under a light microscope. Protoplasts were then centrifuged at 100g for three minutes, supernatant removed, and



re-suspended in MMG (0.4 M mannitol, 15 mM MgCl<sub>2</sub>, and 4 mM MES pH 5.7) to a final concentration between 2.5 and 5 X 10<sup>5</sup> protoplasts/mL.

200 µL of the protoplasts in MMG solution (5 X 10<sup>4</sup> to 1 X 10<sup>5</sup> protoplasts) was used per transfection. The protoplasts were added to 30 µg of plasmid DNA. Then an equal volume of PEG solution [30% (w/v) PEG 4000 (Fluka), 0.1 M CaCl<sub>2</sub>, and 0.2 M mannitol] was added to create a 15% final concentration PEG solution. Protoplasts were incubated for five to 10 minutes at room temperature. After the incubation, 3 mL of W5 solution was slowly added to the side of the tubes to dilute the PEG and stop transfection. The solution was gently rocked to mix and centrifuged at 100g for one minute. The supernatant was removed and the protoplasts were washed in 3 mL W5 then centrifuged at 100g for one minute. Protoplast pellets were re-suspended in 1 mL W5 and placed in 6-well plates. 5% (v/v) calf serum was briefly placed in each well of the plates to prevent sticking directly before the addition of protoplast to the plates. Plates were incubated in plant growth chambers for 16 hours in light at 20°C. After 16 hours incubation, protoplasts were collected and centrifuged at 100g for 2 minutes. The supernatant was removed and the samples were flash frozen in liquid nitrogen and stored at -80°C.

#### 2.10.1 Protoplast Preparation for GUS Assay

100 µL of modified lysis buffer containing 2.5mM Tris-phosphate (pH 7.8) with 1 mM DTT, 2 mM EDTA, 10% (v/v) glycerol, and 1% (v/v) Triton X-100 (Yoo, 2007) was added to the protoplast pellet. Samples were vortexed to rupture protoplasts. Samples

were then placed on ice for five minutes and then centrifuged at 1000 g for two minutes. Ten  $\mu\text{L}$  of the protoplasts in lysis buffer was then used with 100  $\mu\text{L}$  MUG substrate mixture for a GUS assay.

### 2.11 RNA Isolation and Analysis

RNA isolations were performed using RNeasy Plant Mini kits (Qiagen) following the protocol provided by the manufacturer. cDNA was synthesized from 500 ng RNA using SuperScript® III First-Strand Synthesis System (Invitrogen) and the provided oligo dT primers. Samples were then diluted four fold for uses in qPCR. qPCR was performed to amplify and quantify the cDNA. Each well contained 1.0  $\mu\text{L}$  cDNA (from 6.25 ng/ $\mu\text{L}$  RNA), 5  $\mu\text{M}$  of upper primer, 5  $\mu\text{M}$  of lower primer, and 10  $\mu\text{L}$  of 2X Power SYBR Green (Applied Biosystems). The housekeeping gene *AtEF1 $\alpha$*  was amplified using EF1 $\alpha$  forward and EF1 $\alpha$  reverse primers (Table 1) with an initial 2 minutes at 50°C, 10 minutes at 95°C, followed 40 cycles of 15 seconds at 95°C, 60 seconds at 60°C, and a final dissociation step of 15 seconds at 95°C, 30 seconds at 60°C, and 15 seconds at 95°C. *AtERD14* was amplified using *AtERD14* forward and *AtERD14* reverse primers (Table 1) and the same conditions as *AtEF1 $\alpha$* . *AtRD29a* cDNA was amplified using RD29a forward and the RD29a reverse primers (Table 1) with an initial 2 minutes at 50°C, 10 minutes at 95°C, followed 40 cycles of 15 seconds at 95°C, 60 seconds at 63°C, and a final dissociation step of 15 seconds at 95°C, 30 seconds at 60°C, and 15 seconds at 95°C.

## CHAPTER 3. STABLY TRANSFORMED PLANTS' RESPONSE TO COLD STRESS

Several dehydrin promoter constructs were stably transformed into *Arabidopsis thaliana*. Because *A. thaliana* is a cold tolerant plant with a functional cold response pathway, placing a soybean dehydrin promoter controlling a GFP/GUS reporter allows easy and quantitative measurement of the promoter response to a cold stress. A major question I wished to ask was whether the inability for the *GmERD14* to respond to cold is determined by the promoter or by the machinery that recognizes the promoter elements. Based on the reporter response in *A. thaliana*, we could better understand if the soybean dehydrin promoters could contribute to the cold-response efficiency in soybeans. A positive GUS or GFP signal should indicate a functional promoter while a lack of GUS or GFP activity could indicate the promoter is non-functional.

### 3.1 Results

#### 3.1.1 Response of RD29aprom::GFP/GUS to Cold Treatments

The *A. thaliana* dehydrin promoter RD29a is known to be highly up-regulated in *A. thaliana* under cold stress and was used as a positive control in the experiments. RD29aprom::GFP/GUS was transformed into wildtype *A. thaliana*. Floral stem samples

were taken from two month old plants before and after one day cold treatments at 4°C. These were T2 generation plants, and since they were hygromycin resistant, were thus either hemizygous or homozygous individuals for the *RD29a*prom::*GFP/GUS* construct. The reporter GUS ( $\beta$ -glucuronidase) levels were measured using a GUS assay. In the presence of GUS, MUG (4-methylumbelliferyl- $\beta$ -D-glucuronide) is broken down and forms MU (4-methylumbelliferone), a fluorescent compound. The more GUS activity present, the more fluorescence is produced. Continuous monitoring of fluorescence levels over time provided quantitative measurement of the amount of GUS activity in each sample. The value of the linear slope of fluorescence (RFU) increase over time was calculated and the higher slope value indicates greater levels of GUS (Figure 7). Average fold changes were calculated by dividing the slope of the sample after cold treatment by the slope of the sample before cold treatment (Slope 4°C/Slope 20°C). A value above one indicates the sample is cold inducible, a value at one indicates no change in GUS expression after cold, and a value below one indicates a decrease in GUS activity after cold.

Separate stable *RD29a*prom::*GFP/GUS* lines were produced, each line containing a separate transformation event. The lines had a large range of basal (pre-cold) GUS expression levels. Figure 7 indicates the range of basal levels in three of the lines. There was also a large range of cold-inducible GUS activity (Figure 8) [anywhere from a 1.37 to 43 fold increase in GUS activity (Figure 9)]. However, all the lines showed an increase in GUS levels after cold treatment to at least some degree (Figure 9). Month old leaves of

the T3 generation (which in some lines still contained hemizygotes) (Table 3) were also tested before and after cold treatments and also showed an increase in GUS expression after cold treatment (Figure 10).

Whole *RD29a*prom::*GFP/GUS* seedlings of lines H and M were also analyzed. Seedlings were used because they are quickly grown and allow for large sample size. Both lines again showed an increase in GUS expression after a one day cold treatment (Figure 11). Western blots were performed on *RD29a*prom::*GFP/GUS* seedlings using the anti-AtERD14 antibody confirming that the endogenous AtERD14 levels were also increasing in response to the cold treatment (Figure 12). The AtERD14 antibody is known to react with COR47 and ERD10, producing the bands (as indicated) on the western blot. Both COR47 and ERD10 are cold responsive dehydrins and were expected to show increased levels after cold treatment like ERD14 (Figure 12).

Overall, the use of the *RD29a*prom::*GFP/GUS* construct in *A. thaliana* showed that the *RD29a* promoter had higher expression of GUS after cold treatments of leaves, stems, and whole seedlings, which was consistent with its predicted cold-regulated expression.

### 3.1.2 Response of *AtERD14*prom::*GFP/GUS* to Cold Treatments

*AtERD14*prom::*GFP/GUS*, the promoter of the closest *A. thaliana* homologue to the acidic vegetatively expressed soybean dehydrin was also stably transformed into *A. thaliana*. There were only two homozygous *AtERD14*prom::*GFP/GUS* lines created. Two month old *A. thaliana* stems showed no increase in GUS activity in response to cold

stress (Figure 13). Evaluation of *AtERD14* seedlings also showed no increase in GUS activity in response to cold stress (Figure 14).

Western blots were performed on *AtERD14* seedlings using an anti-GFP and anti-ERD14 antibody probed simultaneously. Similar to GUS, the GFP half of the reporter shows no increase in GFP expression in response to cold treatment (Figure 15). However, there was an increase in the endogenous ERD14 expression in response to the 24 hour cold stress (Figure 15).

### 3.1.3 Response of *AtERD14*prom::*AtERD14* in ERD14 KO Background to Cold

#### Treatments

*AtERD14* is known to have increased expression levels in response to cold stress in *A. thaliana*. After *AtERD14*prom::*GFP/GUS* failed to show an increase in the GFP and GUS levels in response to cold treatment, the *AtERD14*prom::*AtERD14* in the *AtERD14* knock out (KO) was examined to verify that the construct introduced on a plasmid could be induced following a cold treatment. As a negative control, the *AtERD14* KO was also transformed with a pCambia1304 vector expressing 35S::*GFP/GUS* only.

Whole seedlings of homozygous *AtERD14*prom::*AtERD14* and with the *AtERD14* KO background with the pCAMBIA1304 vector alone were sampled before and after a 24 hour cold stress at 4°C. A western blot using anti-ERD14 indicated the vector alone transformation did not have detectible levels of ERD14 before or after cold treatment

(Figure 16). All the *AtERD14*prom::*AtERD14* lines tested showed an increase in *AtERD14* protein after a 24 hour cold treatment, though they varied significantly in basal levels (Figure 16).

#### 3.1.4 Response of *GmERD14*prom::*GFP/GUS* to Cold Treatments

*GmERD14*prom::*GFP/GUS* constructs were created and transformed into wildtype *A. thaliana*. Leaf samples of the T3 generation plants were collected before and after 24 hour cold stress at 4°C. Similarly to the *AtERD14* plants, all *GmERD14*prom::*GFP/GUS* lines showed no increase in GUS levels after the cold treatment (Figure 17). Two lines, G and J were analyzed as seedlings by GUS assays and western blots. Both lines showed no increase in GUS activity after cold treatment as seedlings (Figure 11), but did show an increase in endogenous *AtERD14* levels after a cold treatment (Figure 12).

Unlike the *RD29a* control, *GmERD14* promoter does not appear to be sufficient to increase the reporter after cold treatment. Instead, it responds similarly to its homologue *AtERD14* with a constant or lowered GUS expression after cold treatment. A summary of all the promoter constructs and their responses to cold treatments are listed in Table 4.

#### 3.1.5 Response of *AtERD14* Transcript to Cold Treatments

The *AtERD14*prom::*AtERD14* in knocked out *AtERD14* were the only *ERD14* lines to show an increase in protein levels under cold stress, so the *AtERD14* transcript levels

of these lines was analyzed to see if the transcripts had a corresponding increase after cold stress. Whole seedlings were taken before and after 24 hour cold treatment at 4°C (the same time points as used in the protein experiments). RNA was isolated, reverse-transcribed to cDNA, and q-PCR was run using *AtERD14* primers. *AtERD14* transcript levels did show a slight increase in cold stress, when not normalized by their reference gene (Figure 18). However, when normalized by *AtEF1α*, there is no increase in transcript amount after cold stress. The exception was *AtERD14*prom::*AtERD14* line 4-2-4, which showed an insignificant ( $p=0.09$  as determined by a two-tailed T-test) increase in *AtERD14* transcript after the cold treatment. Endogenous ERD14 levels in the *AtERD14*prom::*GFP/GUS* and *AtERD14* knock out transformed with an empty pCambia1304 vector both also showed an increase in transcript levels under cold stress when not normalized (Figure 18). However, the reference gene used (*AtEF1α*) also showed an increase in transcript levels after cold stress (Figure 19). To check that the cold stress was adequate to create a cold response, RD29a transcript levels of the same samples was tested. All samples showed that RD29a transcripts were higher after cold stress both with and without normalization of *AtEF1α* reference gene (Figure 20).



## 3.2 Discussion

### 3.2.1 *AtERD14*, *RD29a*, and *GmERD14* Reporter and Protein Response to Cold

#### Treatments

*AtERD14*prom::*GFP/GUS* was initially planned as a positive transformation and cold responsive control for the *GmERD14*prom::*GFP/GUS*. However, the *AtERD14*prom::*GFP/GUS* plants did not show an increase in GUS activity or GFP protein after cold treatments. Previous studies have shown the endogenous *AtERD14* to be cold inducible in plants at the transcript (Kiyosue, 1994) and protein (Nylander, 2001) level so it seemed likely that there was an error with our construct that was causing it to not act as expected.

Initially, it was hypothesized the reporter was contributing to the lack of GUS and GFP accumulation in the cold. To test this, the promoter of another known cold-inducible gene activated mainly by the ABA independent pathway *RD29a/COR78* (Msanne, 2011) was ligated to the same reporter gene and transformed into *A. thaliana*. *RD29a*prom::*GFP/GUS* plants were tested under the same cold conditions as the *AtERD14*prom::*GFP/GUS* plants. As expected, the *RD29a*prom::*GFP/GUS* plants showed an increase in GUS levels in response to cold treatments. This indicates that the promoter was induced under cold stress to create more of the *GFP/GUS* reporter. The fact that the *RD29a*prom::*GFP/GUS* reporter increased under cold stress indicated that the *GFP/GUS* reporter used was not faulty.

The next potential problem was that the cold treatment was not sufficient to cause a change in *AtERD14*. Western blot analysis of the *AtERD14*prom::*GFP/GUS* using anti-ERD14 indicated that endogenous ERD14 in the plants was up-regulated after cold stress. This shows that the one day cold treatment was adequate to initiate the cold response and increase the amount of gene product.

Another possible explanation for the lack of increase in activity in the *AtERD14*prom::*GFP/GUS* is that the 3' UTR or coding region intron is necessary for the promoter to respond to cold, and because this is not in the construct, the promoter is unable to cause a response in the reporter. The need for introns to cause gene expression is seen in maize alcohol dehydrogenase 1 (*ADH1*). *ADH1* constructs lacking all nine introns were expressed at levels 50 to 100 times less than constructs that did contain the introns (Callis, 1987). Another possibility is that the promoter construct did not go far enough upstream from the start codon to contain all the necessary elements to activate the gene properly under cold stress. Although the *AtERD14* promoter construct went 2500 bp upstream of the start codon, in mammalian cells, the *Kit* enhancer is located 150 kb upstream of the promoter (Berrozpe, 2013). If either of these possibilities is true, then the *AtERD14*prom::*AtERD14* in the ERD14 KO (which uses the same promoter sequence as the *AtERD14*prom::*GFP/GUS*) would also fail to show an increase in ERD14 levels after cold treatment. The vector alone transformation shows no ERD14 activity under any treatment, indicating that endogenous *AtERD14* truly was knocked out prior to inserting the *AtERD14*prom::*AtERD14*. Therefore, any

ERD14 presence in the *AtERD14*prom::*AtERD14* lines may be attributed to the introduced promoter construct.

Contrary to what one would expect (if the appropriate *ERD14* sequences were missing), the ERD14 protein from the *AtERD14*prom::*AtERD14* plants was increased after the cold stress. Up-regulation of ERD14 in the *AtERD14*prom::*AtERD14* in the *AtERD14* KO indicates that the *AtERD14* promoter used in the constructs is sufficient in the context of the coding region for ERD14 (even though it lacks the 3' UTR and the short intronic sequence).

The *AtERD14* promoter only functioned as expected when we attached the proper protein coding region to the construct. This could indicate that some transcriptional regulation occurs for these dehydrins, where it is necessary to have both the promoter and coding region elements to accumulate the RNA and the protein. For example, it is possible that an activating complex binds to both the promoter and coding region to start transcription and without the proper coding region it cannot activate the promoter. An example of this type of regulation occurs in the herpes simplex virus. The herpes simplex virus early glycoprotein D gene contains three ICP4 activation binding sites. Two of these binding sites are located in the promoter sequence, but the final binding site is located in the coding region, and all three binding sites are used to stimulate transcription (Tedder, 1989).

Another possibility is that auto-regulation occurs where the *AtERD14* protein binds to its own promoter in order to activate the gene. This type of regulation is seen in the eye where the Pax-QNR protein directly binds to the *Pax-QNR* promoter to activate

it (Plaza, 1993). Another form of auto-regulation that could occur is the AtERD14 protein could bind to its own RNA to regulate its activity. HSP70 protein is able to bind directly to its mRNA to regulate its expression level (Balakrishnan, 2006). This is especially interesting because *HSP70* and *AtERD14* share another quality in that they both function to protect against damage after abiotic stress and can act to keep other proteins folded properly after a stress.

The results could also mean that transcriptional regulation occurs where the AtERD14 protein is stabilized after exposure to cold. For example, it could be that the AtERD14 protein turnover rate is dramatically reduced under cold stress and because the GFP/GUS reporter did not contain elements that a cold stress stabilized, it did not appear to accumulate in response to cold. Whichever (perhaps a combination of several) answer is correct, there seems to be a clear difference in the regulation of the *RD29a* gene than there is in the *ERD14* dehydrin.

### 3.2.2 AtERD14 Transcript Has a Slight Response to Cold

Although the ERD14 protein increased in response to cold in the *AtERD14prom::AtERD14* plants, the ERD14 transcript showed only a slight increase in response to cold treatments when not normalized by a reference gene. The *AtERD14prom::GFP/GUS* also showed the same expression pattern in endogenous AtERD14 after cold treatments, indicating that our construct is reacting similarly as wild type. When ERD14 was normalized by the reference gene, there was no increase in ERD14 transcript, except in line 4-2-4, which had a slight, but statistically insignificant

increase in transcript. However, the lack of transcript cold inducibility could be due to the fact that the reference gene used showed increased transcript levels after cold treatment, indicating that it is an inappropriate reference gene in these experiments. Kiyosue (1994) looked at the ERD14 transcript and found an increase after cold treatments, however this conclusion was reached without normalizing by a reference gene, consistent with results discussed here. Nylander et al (2001) looked at various dehydrins, including *ERD14*, and the transcript levels of ERD14 in leaf and stems of eight-week old *A. thaliana* after a three day cold treatment appears to be the same as the control levels. Likewise, Seki et al (2001) also saw that there was no significant up-regulation of ERD14 transcript under cold stress ( $1.5 \pm 0.4$  fold change). All these results combined seem to indicate that any possible transcript upregulation of AtERD14, if it does occur, would be very slight.

The absence of an increase in transcript levels when normalized by AtEF1 $\alpha$  under cold stress despite an increase in protein levels could simply be a timing issue. Our lab has seen several dehydrins cycle transcript levels throughout the day, with a peak four hours after cold activation followed by a decrease in transcript level (Yamasaki and Randall lab, unpublished) (uniprot.org). A similar phenomenon could be happening with the ERD14. The transcript could be peaking early on then dropping back down towards base level after 24 hours in a cold treatment. However, the protein would be present at greater levels at the 24 hour mark because its peak in activity is delayed and only formed after the transcript is made. On the other hand, RD29a transcript increased after cold treatments even after normalization because the transcript was so strongly

induced by the cold treatment. This indicates that the cold treatment was sufficient to cause a cold response, even if it did not show the response predicted in the *AtERD14*.

### 3.3 Future Plans

I hypothesize that the *GmERD14* promoter will act in the same way as the *AtERD14* promoter, and to test this, a *GmERD14*prom::*GmERD14* construct transformed into *Arabidopsis thaliana* could be created. If it is functional, then it indicates that the soybean dehydrin promoters are functional, and the defect in the cold tolerance pathway in soybean lies elsewhere in the machinery. A defect in the machinery could include a negative regulator that isn't properly turned off under cold stress, similarly to how HOS1 binds to ICE1 to prevent it from activating CBF (Thomashow, 2010).

If the *GmERD14*prom::*GmERD14* construct in *A. thaliana* is not cold upregulated, which suggests that ineffective promoters may be the cause for soybean's cold intolerance. I have now shown *AtRD29a*::GFP/GUS is a functional promoter in *A. thaliana* and under cold stress has increased levels of the GUS reporter. If this construct causes an increase in GUS activity after a cold stress in the soybean, then it would show the machinery works in soybean (and thereby indicates that the problem lies in the native soybean promoters). If this construct is not affected by cold stress, it would indicate a problem in the machinery and not the promoters in soybean.

In interest of looking at the promoter and coding region connection a *GmERD14*prom::*AtERD14* and *AtERD14*prom::*GmERD14* transformed into *A. Thaliana* could be created. It will be interesting to see whether the *GmERD14* coding region is

similar enough to *AtERD14* coding region that it will have increased expression after a cold stress when hooked up to an *AtERD14* promoter, or if each promoter needs to be next to its own coding region in order to get the proper cold up-regulation response. It will also be interesting to see if the *GmERD14*prom::*AtERD14* is functional but not the *AtERD14*prom::*GmERD14*, perhaps indicating that *GmERD14* coding region is missing the elements to properly stabilize the translated protein after a cold stress.

I hypothesize that there is some complex that must bind to both the promoter and coding region of the *ERD14* in order to activate the gene to start transcription. In order to test this, we could make several versions of the *AtERD14* coding region fused with a GFP/GUS reporter with different sections of the *AtERD14* coding region removed in order to see which section is needed to cause a response in the reporter after cold stress, and thus the cold-inducible accumulation of ERD14.

It has been shown that *A. thaliana* grown under shorter days will have an increased freezing tolerance and will also have increased expression of *CBF* and other genes induced by the ABA independent pathway (Lee, 2012). All the experiments performed for this thesis were conducted under long day (18h) conditions. The depression of cold inducible genes under long days means that significant changes in *AtERD14* activity could be missed simply because experiments were performed under suboptimal daylight conditions.

## CHAPTER 4. METHODOLOGY OF PROTOPLAST TRANSFECTION AND GUS ASSAY

In order to shortcut the process of making stably transformed plants, a transient transformation assay using protoplasts was used. Following Wu et al (2009) method of protoplast transformation, approximately one month old wildtype *A. thaliana* leaf protoplasts were generated by digesting cell walls using cellulose and macerozyme. The 35S::GFP/GUS construct (30  $\mu\text{g}/\mu\text{L}$ ) was introduced into  $1 \times 10^5$  protoplasts using 15% final polyethylene glycol. Protoplasts were incubated for 16 hours at 20°C. GUS activity, by measuring the accumulation of MU, was measured continuously at 360nm excitation and 460nm emission over one hour on a Spectramax M2® Pro 5 in a 96 well format.

### 4.1 Results

#### 4.1.1 Wavelengths Used to Measure GUS Assay

In order to best observe MU activity, optimal emission and excitation wavelength using the lysis buffer must be obtained for the GUS assay. Following Fior et al (2009), samples of MUG and lysis buffer were prepared with and without MU. To determine the optimal emission wavelength, the excitation wavelength was set at



350nm and the level of fluorescence was measured at emission wavelengths between 350 and 500nm with readings taken every 10nm (Figure 21). The 460nm emission wavelength had the largest difference in fluorescence values between the samples with and without MU (Figure 21). To determine optimal excitation wavelength, the emission wavelength was set at 453nm and the amount of fluorescence was measured at excitation wavelengths between 300 and 400nm with readings done every 10 nm (Figure 22). The 360nm excitation wavelength had the largest difference in fluorescence values between the two samples (Figure 22).

#### 4.1.2 Linear Range of GUS Assay

To determine the linear range of MU detectability, different concentrations of MU were added into the standard assay mixture. The fluorescence (RFU) at each concentration was measured and plotted to show the linear range of activity (Figure 23). Linear fluorescence readings occurred until past 20,000 RFU. At 25,000 RFU, the fluorescence response becomes clearly non-linear (Figure 24).

To verify that the linear range used was appropriate for actual samples, dilution series of whole plant extracts of AtERD14prom::GFP/GUS was performed. These samples contained GUS so here the slope of MU activity produced via the GUS substrate was plotted to show linearity (Figure 25).

#### 4.1.3 Minimal Amount of Protoplasts

The suggested range of protoplasts varies from  $2 \times 10^4$  to  $1 \times 10^5$  protoplasts per transfection (Yoo, 2007; Wu, 2009). This translates to roughly 2,000 to 10,000 protoplasts per GUS assay. Initial use of 2,000 protoplasts per GUS assay showed undetectable levels of MU activity in transformed protoplasts (Figure 26). Increasing protoplasts concentration to 4,000 protoplasts per GUS assay showed linear MU activity levels (Figure 26).

#### 4.1.4 Transient Transformation of Protoplasts

Wildtype *A. thaliana* protoplasts were isolated and transformed with different promoter reporter constructs. *AtERD14prom::GFP/GUS* (Figure 26), *RD29aprom::GFP/GUS* (Figure 27) and *35S::GFP/GUS* (Figure 28) showed detectable GUS activity when transformed into wildtype *A. thaliana* protoplasts. However, when a cold treatment of any type was performed of the *RD29aprom::GFP/GUS* (the cold positive control), the amount of GUS activity was decreased. Table 5 shows a list of some of the attempted cold treatments of transformed protoplasts. Cold treatments were attempted before and after PEG transformation and for various lengths of time. All cold treatments of protoplasts resulted in a decrease in the amount of reporter activity as opposed to the expected increase.

## 4.2 Discussion

An increasing linear range of RFU is necessary to obtain readable GUS activity levels. At least 4,000 protoplasts per GUS assay were needed in order to get a reliable and readable response of GUS activity. Although protoplasts at lower concentrations were readily transformed (as verified by visualizing GFP by fluorescent microscopy), the amount of GUS reporter activity was too low for our plate reader to get a reading. Emission and excitation scans indicate that the optimal emission wavelength for the lysis buffer used is 460nm and the optimal excitation wavelength is 360nm. At 25,000 RFU, the fluorescence is saturated, so the cut off for maximum fluorescent used in all experiments was 20,000 RFU.

Although we were able to transform all the constructs into wildtype, we were never able to successfully have protoplasts survive and upregulate *RD29aprom::GFP/GUS* after the cold treatments. Because cold up-regulation was never successfully measured, we had to resort to stably transforming whole plants to get meaningful results. However, in further experiments where cold treatments are not needed; the protoplast transient transformation assay can be used. Finding the parameters to run a GUS assay allowed us to use this assay on whole plants to detect their GUS activity.

## 4.3 Future Plans

In the future, our lab can use the protoplast transformation assay to look at genes that do not require cold inducibility. One possible way to circumvent a cold treatment

on the protoplasts could be to perform a double transformation with our genes of interest and *CBF* (an up-stream transcription factor) to see if *CBF* can be used in lieu of a cold treatment to up-regulate potential cold-responsive promoters.

## REFERENCES

## REFERENCES

- Alsheikh, M. K., B. J. Heyen and S. K. Randall (2003). "Ion binding properties of the dehydrin ERD14 are dependent upon phosphorylation." Journal of Biological Chemistry **278**(42): 40882-40889.
- Alsheikh, M. K., J. Svensson and S. K. Randall (2005). "Phosphorylation regulated ion-binding is a property shared by the acidic subclass dehydrins." Plant, Cell and Environment **28**: 1114-1122.
- Balakrishnan, K. and A. Maio (2006). "Heat shock protein 70 binds its own messenger ribonucleic acid as part of a gene expression self-limiting mechanism." Cell Stress Chaperones **11**(1): 44-50.
- Berrozpe, G., G. O. Bryant, K. Warpinski and M. Ptashne (2013). "Regulation of a mammalian gene bearing a CpG island promoter and a distal enhancer." Cell Reports **4**(3): 445-453.
- Black, R., H. Alderman, Z. Bhutta, S. Gillespie, L. Haddad, S. Horton, A. Lartey, V. Mannar, M. Ruel, C. Victoa, S. Walker and P. Webb (2013). "Maternal and child nutrition: building momentum for impact." The Lancet **382**(9890): 372-375.
- Bradford, M. M. (1976). "A rapid and sensitive method for the quantitation of microgram quantities of protein utilizing the principle of protein-dye binding." Analytical Biochemistry **72**: 248-254.
- Callis, J., M. Fromm and V. Walbot (1987). "Introns increase gene expression in cultured maize cells." Genes & Development **1**(10): 1183-1200.

- Chinnusamy, V., K. Schumaker and J. K. Zhu (2004). "Molecular genetic perspectives on cross-talk and specificity in abiotic stress signalling in plants." Journal of Experimental Botany **55**(395): 225-236
- Chinnusamy, V., J. Zhu and J.-K. Zhu (2007). "Cold stress regulation of gene expression in plants." Trends in Plant Science **12**(10): 445-451.
- Ciarmiello, L. F., P. Woodrow, A. Fuggi, G. Pontecorvo and P. Carillo (2011). "Plant Genes for Abiotic Stress, Abiotic Stress in Plants - Mechanisms and Adaptations." 14 March 2013. <http://www.intechopen.com/books/abioticstress-in-plants-mechanisms-and-adaptations/plant-genes-for-abiotic-stress>.
- Close, T. J. (1997). "Dehydrins: A commonality in the response of plants to dehydration and low temperature." Physiologia Plantarum **100**: 291-296.
- Davik, J., G. Koehler, B. From, T. Torp, J. Rohloff, P. Eidem, R. C. Wilson, A. Sønsteby, S. K. Randall and M. Alsheikh (2013). "Dehydrin, alcohol dehydrogenase, and central metabolite levels are associated with cold tolerance in diploid strawberry (*Fragaria* spp.)." Planta **237**: 265-277.
- FAO (2013). The multiple dimensions of food security. The State of Food Insecurity in the World. Rome, Food and Agricultural Organization of the United Nations.
- Fior, S., A. Vianelli and P. D. Gerola (2009). "A novel method for fluorometric continuous measurement of  $\beta$ -glucuronidase (GUS) activity using 4-methyl-umbelliferyl- $\beta$ -D-glucuronide (MUG) as substrate." Plant Science **176**: 130-135.
- Gilmour, S. J., R. K. Hajela and M. F. Thomashow (1988). "Cold Acclimation in *Arabidopsis thaliana*." Plant Physiology **87**(3): 745-750.
- Hanin, M., F. Brini, C. Ebel, Y. Toda, S. Takeda and K. Masmoudi (2011). "Plant dehydrins and stress tolerance: versatile proteins for complex mechanisms." Plant Signaling & Behavior **6**(10): 1503-1509.

- Hara, M., M. Fujinaga and T. Kuboi (2004). "Radical scavenging activity and oxidative modification of citrus dehydrin." Plant Physiology and Biochemistry **42**(7-8): 657-662.
- Hara, M., M. Fujinaga and T. Kuboi (2005). "Metal binding by citrus dehydrin with histidine-rich domains." Journal of Experimental Botany **56**(420): 2695-2703.
- Harrison, S. J., E. K. Mott, K. Parsley, S. Aspinall, J. C. Gray and A. Cottage (2006). "A rapid and robust method of identifying transformed *Arabidopsis thaliana* seedlings following floral dip transformation." Plant Methods **2**: 19.
- Houde, M., R. S. Dhindsa and F. Sarhan (1992). "A molecular marker to select for freezing tolerance in Gramineae." Molecular and General Genetics **234**(1): 43-48.
- Kiyosue, T., K. Yamaguchi-Shinozaki and K. Shinozaki (1994). "Characterization of two cDNAs (ERD10 and ERD14) corresponding to genes that respond rapidly to dehydration stress in *Arabidopsis thaliana*." Plant & Cell Physiology **35**(2): 225-231.
- Koag, M. C., R. D. Fenton, S. Wilkens and T. J. Close (2003). "The binding of maize DHN1 to lipid vesicles. Gain of structure and lipid specificity." Plant Physiology **131**(1): 309-316.
- Kovacs, D., E. Kalmar, Z. Torok and P. Tompa (2008). "Chaperone activity of ERD10 and ERD14, two disordered stress-related plant proteins." Plant Physiology **147**: 381-390.
- Laemmli, U. K. (1970). "Cleavage of structural proteins during the assembly of the head of bacteriophage T4." Nature **227**(5259): 680-685.
- Lee, C.-M. and M. F. Thomashow (2012). "Photoperiodic regulation of the C-repeat binding factor (CBF) cold acclimation pathway and freezing tolerance in *Arabidopsis thaliana*." Proceedings of the National Academy of Sciences **109**(37): 15054-15059.



- Martinez-Trujillo, M., V. Limones-Briones, J. L. Cabrera-Ponce and L. Herrera-Estrella (2004). "Improving transformation efficiency of *Arabidopsis thaliana* by modifying the floral dip method." Plant Molecular Biology Reporter **22**(1): 63-70.
- McKhann, H. I., C. Gery, A. Berard, S. Leveque, E. Zuther, D. K. Hinch, S. De Mita, D. Brunel and E. Teoule (2008). "Natural variation in CBF gene sequence, gene expression and freezing tolerance in the Versailles core collection of *Arabidopsis thaliana*." BMC Plant Biology **8**: 105.
- Miura, K., J. B. Jin, J. Lee, C. Y. Yoo, V. Stirm, T. Miura, E. Ashworth, R. Bressan, D.-J. Yun and P. Hasegawa (2007). "SIZ1-Mediated Sumoylation of ICE1 Controls CBF3/DREB1A Expression and Freezing Tolerance in *Arabidopsis*." The Plant Cell **19**: 1403-1414.
- Msanne, J., J. Lin, J. M. Stone and T. Awada (2011). "Characterization of abiotic stress-responsive *Arabidopsis thaliana* RD29A and RD29B genes and evaluation of transgenes." Planta **23**: 97-107.
- Murashige, T. and F. Skoog (1962). "A Revised Medium for Rapid Growth and Bio Assays with Tobacco Tissue Cultures." Physiologia Plantarum **15**(3): 473-497.
- Narusaka, Y., K. Nakashima, Z. K. Shinwari, Y. Sakuma, T. Furihata, H. Abe, M. Narusaka, K. Shinozaki and K. Yamaguchi-Shinozaki (2003). "Interaction between two cis-acting elements, ABRE and DRE, in ABA-dependent expression of *Arabidopsis* rd29A gene in response to dehydration and high-salinity stresses." The Plant Journal **34**: 137-148.
- Nylander, M., J. Svensson, E. T. Palva and B. V. Welin (2001). "Stress-induced accumulation and tissue-specific localization of dehydrins in *Arabidopsis thaliana*." Plant Molecular Biology **45**: 263-279.
- O'Brien, J., A. Daudi, V. Butt and G. P. Bolwell (2012). "Reactive oxygen species and their role in plant defence and cell wall metabolism." Planta **236**: 765-779.
- Plaza, S., C. Dozier and S. Saule (1993). "Quail Pax-6 (Pax-QNR) encodes a transcription factor able to bind and trans-activate its own promoter." Cell Growth & Differentiation **4**(12): 1041-1050.

Puhakainen, T., M. W. Hess, P. Makela, J. Svensson, P. Heino and E. T. Palva (2004). "Overexpression of multiple dehydrin genes enhances tolerance to freezing stress in *Arabidopsis*." Plant Molecular Biology **54**(5): 743-753.

Qin, F., Y. Sakuma, L.-S. P. Tran, K. Maruyama, S. Kidokoro, Y. Fujita, M. Fujita, T. Umezawa, Y. Sawano, K.-i. Miyazono, M. Tanokura, K. Shinozaki and K. Yamaguchi-Shinozaki (2008). "*Arabidopsis* DREB2A-Interacting Proteins Function as RING E3 Ligases and Negatively Regulate Plant Drought Stress-Response Gene Expression." The Plant Cell **20**: 1693-1707.

Qin, F., K. Shinozaki and K. Yamaguchi-Shinozaki (2011). "Achievements and challenges in understanding plant abiotic stress responses and tolerance." Plant Cell and Physiology **52**(9): 1569-1582.

Rorat, T. (2006). "Plant Dehydrins - Tissue Location, Structure and Function." Cellular & Molecular Biology Letters **11**: 536-556.

Seki, M., M. Narusaka, H. Abe, M. Kasuga, K. Yamaguchi-Shinozaki, P. Carninci, Y. Hayashizaki and K. Shinozaki (2001). "Monitoring the Expression Pattern of 1300 *Arabidopsis* Genes under Drought and Cold Stresses by Using a Full-Length cDNA Microarray." The Plant Cell **13**: 61-72.

Shinozaki, K. and K. Yamaguchi-Shinozaki (2000). "Molecular responses to dehydration and low temperature: differences and cross-talk between two stress signaling pathways." Current Opinion in Plant Biology **3**(3): 217-223.

Smith, P., P. J. Gregory, D. van Vuuren, M. Obersteiner, P. Havlik, M. Rounsevell, J. Woods, E. Stehfest and J. Bellarby (2010). "Competition for land." Philosophical Transactions of the Royal Society of London, Series B, Biological Sciences **365**(1554): 2941-2957.

Tedder, D., R. Everett, K. Wilcox, P. Beard and L. Pizer (1989). "ICP4-Binding Sites in the Promoter and Coding Regions of the Herpes Simplex Virus gD Gene Contribute to Activation of In Vitro Transcription by ICP4." Journal of Virology **63**(6): 2510-2520.

Thomashow, M. F. (2010). "Molecular Basis of Plant Cold Acclimation: Insights Gained from Studying the CBF Cold Response Pathway." Plant Physiology **154**: 571-577.

- Wu, F. H., S. C. Shen, L. Y. Lee, S. H. Lee, M. T. Chan and C. S. Lin (2009). "Tape-Arabidopsis Sandwich - a simpler Arabidopsis protoplast isolation method." Plant Methods **5**: 16.
- Yamasaki, Y., G. Koehler, B. J. Blacklock and S. K. Randall (2013). "Dehydrin expression in soybean." Plant Physiology and Biochemistry **70**: 213-220.
- Yoo, S.-D., Y.-H. Cho and J. Sheen (2007). "*Arabidopsis* mesophyll protoplasts: a versatile cell system for transient gene expression analysis." Nature Protocols **2**(7): 1565-1572.
- Zhang, X., R. Henriques, S.-S. Lin, Q.-W. Niu and N.-H. Chua (2006). "*Agrobacterium*-mediated transformation of *Arabidopsis thaliana* using the floral dip method." Nature Protocols **1**: 641-646.

## TABLES

Table 1: List of all primer sequences used and their targets

Abbreviated name indicates how the primer is referred to in the text while the primer name is the full primer name. Primer concentrations are 5  $\mu$ M, except for primers used for sequencing which had a concentration of 3  $\mu$ M.

Abbreviated Name	Primer Name	Target	Sequence (5' to 3')
GmERD14 forward	Glyma04g01130prom-CU-2815	GmERD14	TTCGTTTCATGAGACTCACACA
GmERD14 reverse	GmTC203260 lower1	GmERD14	AAAACAAAGCACACCACAATCAT
GmERD14 BamHI	PromBamHI	BamHI/ GmERD14	GGATCCATGTACCAATAAATTAG GTTCACATC
GmERD14 NcoI	StartNcoI	NcoI/ GmERD14	CCATGGTGTATTAGTGAAGTGAA GTGAT
RD29a BamHI	AtRD29A-1480BamHI	BamHI/ AtRD29a	GGATCCTCTGTTTGTGAACCTTGA TGT
GUS reverse	pCambia1304+2134GUS-L	GUS	AATAACGGTTCAGGCACAGC
GUS forward	pCambia1304+1170GUS-U	GUS	GGTGATTACCGACGAAAACG
35S forward	pCambia1304-35S sequencing	35S	CGCACAATCCCACTATCCTT
EF1 $\alpha$ forward	Atef1 $\alpha$ +354qPCR-U	AtEF1 $\alpha$	CACCACTGGAGGTTTTGAGG
EF1 $\alpha$ reverse	Atef1 $\alpha$ +572qPCR-L	AtEF1 $\alpha$	TGGAGTATTTGGGGGTGGT
AtERD14 forward	At1g76180.1 Real U	ERD14	TCATATTTAGAGCCGGAGCC
AtERD14 reverse	At1g76180.1 Real L	ERD14	AACTGTCGCTTCGGTGAAGCT
RD29a forward	AtRD29a+311qPCR-U	RD29a	GCACCAGGCGTAACAGGTAAC
RD29a reverse	AtRD29a+467qPCR-L	RD29a	AAACACCTTTGTCCCTGGTGG
GFP reverse	pCambia1304-mgfp 5 Reverse	GFP	TGCCATTAACATCACCATC
GmERD14 sequencing forward	Glyma04g01130-SeqU-1655	GmERD14	CTCGCACCTCCTCAAGCTAT
GmERD14 sequencing reverse1	Glyma04g01130-SecL-416	GmERD14	AACGAAGTTTCCATTTAATTATAA GAA
GmERD14 sequencing reverse2	Glyma0401130-SecL-1261	GmERD14	TGTTTTCAATTGTCTTTTGTATCG

Table 2: Hygromycin resistance of T2 lines used in experiments

Separate letters represent separate lines, each of which represents a separate transformation event. Values indicate the percent of seedlings per plate that had hygromycin B resistance. A chi-square test was performed over the T2 seedlings. Expected values for the chi-square are 3:1 ratio of resistant: sensitive seedlings for hygromycin B. Lines that passed the chi-square test are highlighted in red. Those lines that passed the chi-square test (especially when one hundred seedlings were scored) are most likely to contain a single insert. Lines that did not pass the chi-square test and had a higher than predicted percent of seedlings with hygromycin resistance likely contained multiple vector inserts. (A) At least one hundred seedlings were scored per plant line. (B) Thirty seedlings were scored per line. Seeds that did not germinate were not counted in the total number of seedlings.

(A)

GmERD14 Line	Percent HygroB Resistant	AtRD29a Line	Percent HygroB Resistant
G	92.7%	H	94.3%
J	77.3%	K	75.9%
K	75.0%	M	58.8%

(B)

GmERD14 Line	Percent HygroB Resistant	AtRD29a Line	Percent HygroB Resistant
A	75.5%	C	42.3%
B	92.3%	E	85.7%
C	88.5%	F	60.7%
D	85.7%	G	40.7%
E	70.0%	H	90.0%
G	89.3%	I	69.0%
H	88.5%	K	55.6%
I	36.0%	L	62.5%
J	66.7%	M	73.3%
K	72.0%		
L	92.0%		

Table 3: Hygromycin resistance of T3 lines used in experiments

Six plants per line were grown in the T2 generation (numbered 1-6). Seeds were collected from each T2 plant and T3 seedlings were grown on plates containing hygromycin B. Values indicate the percent of seedlings per plate that had hygromycin B resistance. (A) At least one hundred seedlings were scored. (B) Thirty seedlings were scored per plant. Seeds that did not germinate were not counted in the total number of seedlings. Values in red indicated seed stocks used for T3 generation experiments.

(A)

GmERD14 Line	Percent HygroB Resistant	AtRD29a Line	Percent HygroB Resistant
G.6	92.4	H.6	90
J.4	96.9	K.2	69.2
K.5	98.4	M.3	87.3

Table 3 continued.

(B)

GmERD14 Line	Percent HygroB Resistant	AtRD29a Line	Percent HygroB Resistant
C.1	75.0%	F.1	0%
<b>C.2</b>	<b>80.8%</b>	F.2	53.6%
C.3	70.4%	F.3	0%
C.4	64.0%	<b>F.4</b>	<b>60.0%</b>
C.5	82.8%	F.5	39.3%
C.6	80.8%	F.6	35.7%
G.1	96.6%	H.1	89.7%
G.2	90.0%	H.2	75.9%
G.3	89.3%	H.3	56.5%
G.4	80.0%	H.4	82.1%
G.5	96.2%	H.5	70.0%
<b>G.6</b>	<b>96.7%</b>	<b>H.6</b>	<b>89.3%</b>
J.1	45.8%	<b>I.1</b>	<b>89.3%</b>
J.2	75.9%	I.2	76.7%
J.3	70.0%	I.3	87.5%
<b>J.4</b>	<b>100%</b>	I.4	87.5%
J.5	92.6%	I.5	61.5%
J.6	90.0%	I.6	60.0%
K.1	69.0%	K.1	60.7%
K.2	72.4%	<b>K.2</b>	<b>75.0%</b>
K.3	63.0%	K.3	56.0%
K.4	71.4%	K.4	57.1%
<b>K.5</b>	<b>89.3%</b>	K.5	58.3%
K.6	60.7%	K.6	50.0%
L.1	82.1%	M.1	66.7%
L.2	83.3%	M.2	60.7%
<b>L.3</b>	<b>86.2%</b>	<b>M.3</b>	<b>92.9%</b>
L.4	82.6%	M.4	57.1%
L.5	64.3%	M.5	82.8%
L.6	84.6%	M.6	57.7%



Table 4: Summary of promoter responses to cold treatment

Summary table of stably transformed *A. thaliana* T-3 plant constructs and their activity in response to 24 hour cold treatments at 4°C. Lines tested that support conclusions are listed under the results. Lines highlighted in red are homozygous seed populations. N.D. is not determined.

Promoter	Coding	GUS Activity (GUS Assay)	Protein (Western)	Transcript (qRT-PCR)
<i>AtERD14</i>	<i>AtERD14</i>	n/a	↑ <i>AtERD14</i> (Lines: 3-1-4, 3-1-6, 4-2-4)	Slight ↑ <i>AtERD14</i> (Lines: 3-1-4, 3-1-6, 4-2-4)
<i>AtERD14</i>	GFP/GUS	No Increase GUS (Lines: 1-1-4, 2-3-5)	No Increase GFP (Line: 1-1-4) ↑ Endogenous <i>AtERD14</i> (Line: 1-1-4)	Slight ↑ Endogenous <i>AtERD14</i> (Line: 1-1-4)
<i>GmERD14</i>	GFP/GUS	No Increase GUS (T2 lines: L, G, H, J, A, C) (T.3 lines: G.6, J.4, C.2, K.5)	↑ Endogenous <i>AtERD14</i> (T.3 lines: G.6, J.4)	N.D.
<i>RD29a</i>	GFP/GUS	↑ GUS (T.2 lines: I, K, F, H, M) (T.3 lines: I.1, K.2, F.4, M.3, H.6)	↑ Endogenous <i>AtERD14</i> (T.3 lines: H.6 and M.3)	N.D.

Table 5: List of attempted cold treatments performed on transformed protoplasts. The additional treatment (if performed) occurred directly after the treatment performed after transformation (i.e. 4 hours at 4°C followed by 20 hours at 20°C in the fourth experiment).

Time in Cold (4°C) Before Transformation	Treatment Directly After Transformation	Additional Treatment (optional)
1 hour	16 hours 20°C	
0 hours	16 hours 4°C	
0 hours	18 hours 4°C	
0 hours	4 hours 4°C	20 hours 20°C
0 hours	3 hours 4°C	14 hours 20°C
0 hours	19 hours 20°C	2 hours 4°C

## FIGURES

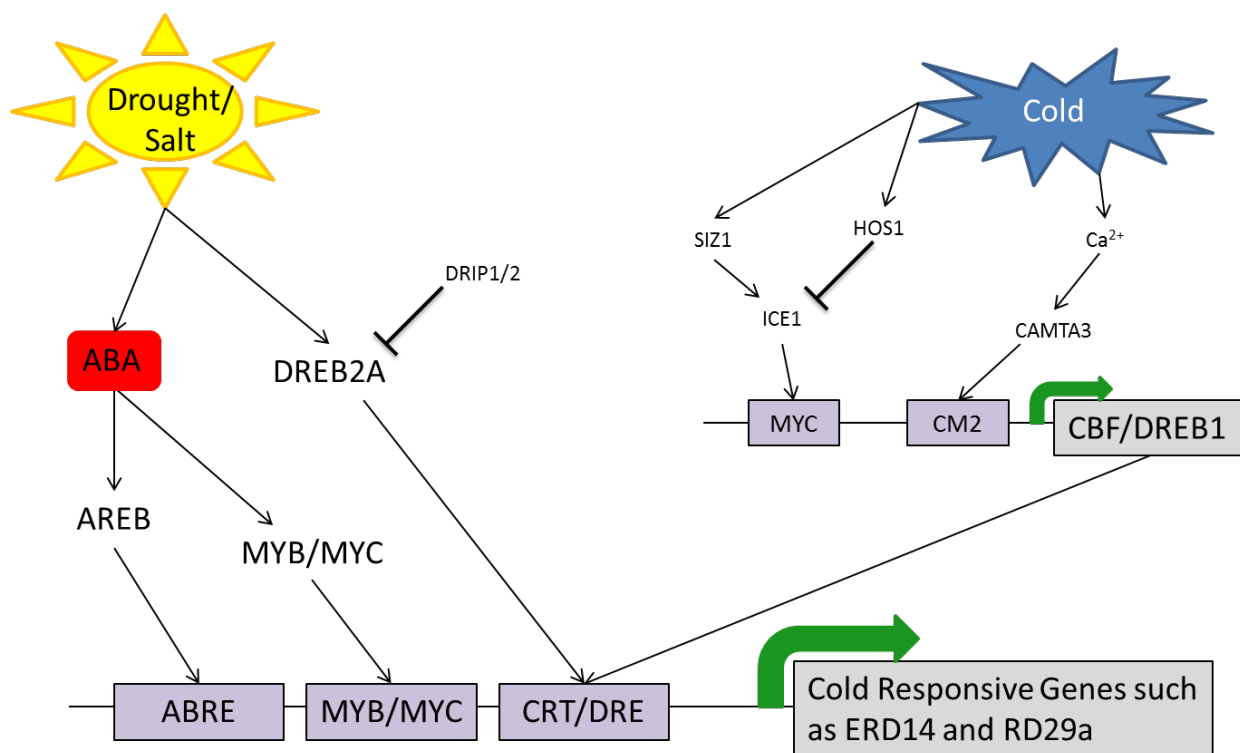


Figure 1: ABA dependent and independent pathways in cold tolerant *A. thaliana*. Drought and high salinity causes an increase in ABA, which causes an increase in MYB/MYC and AREB transcription factors. AREB bind to ABRE sequences and MYB/MYC bind to MYB/MYC sequences in cold responsive (COR) gene promoters. Drought and high salinity also activate DREB2A, allowing it to bind to CRT/DRE sequences in COR promoters. When unstressed, DRIP1/2 will ubiquitinate DREB2A. Cold activates HOS1 and SIZ1. SIZ1 sumoylates ICE1, allowing it to bind to the MYC region in the CBF promoter. HOS1 works in opposition to SIZ1 and degrades ICE1. CBF binds to CRT/DRE sequences in COR promoters to activate the genes. Ca<sup>2+</sup> activates CAMTA3, allowing it to bind to CM2 to increase CBF expression. Model is based on ABA dependent and independent model created by Yuji Yamasaki (not published).

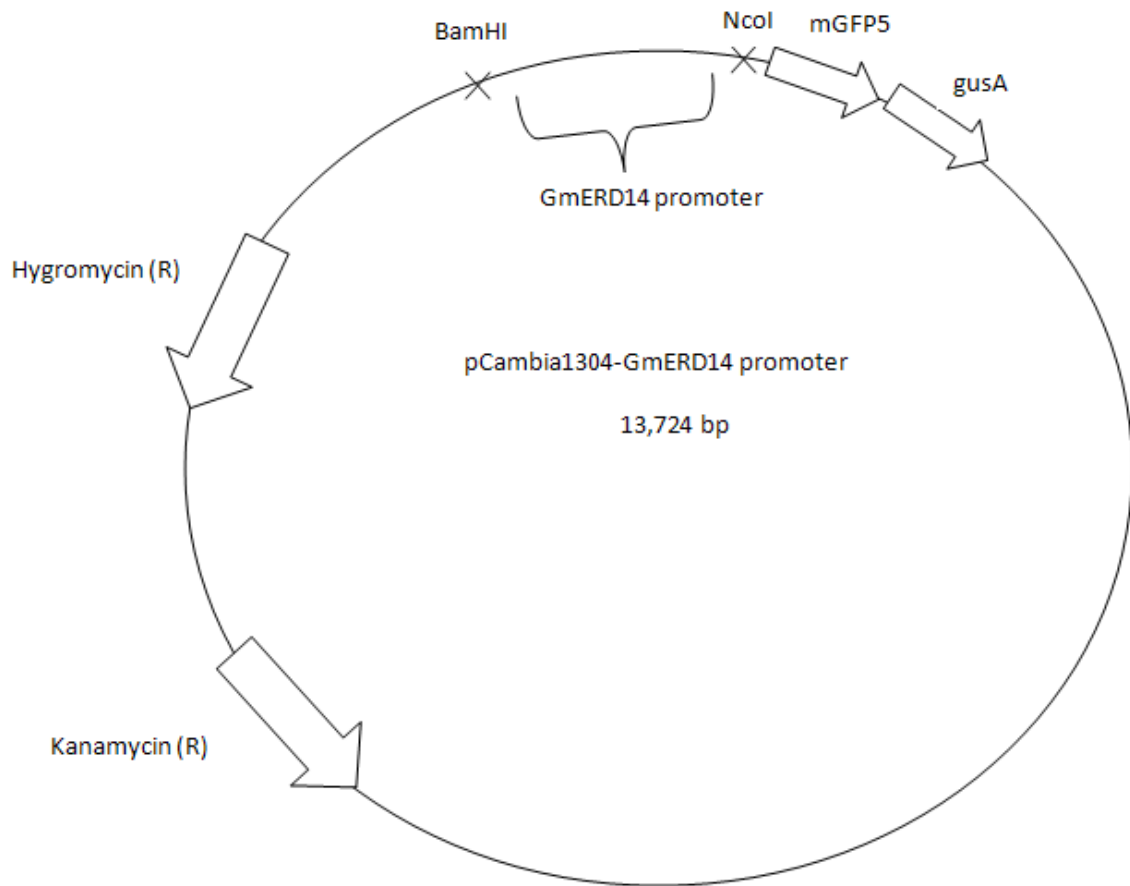


Figure 2: *GmERD14*prom::GFP/GUS in pCambia 1304. *GmERD14* promoter was inserted into BamHI and NcoI in the pCambia1304 vector to create the *GmERD14*prom::GFP/GUS construct.

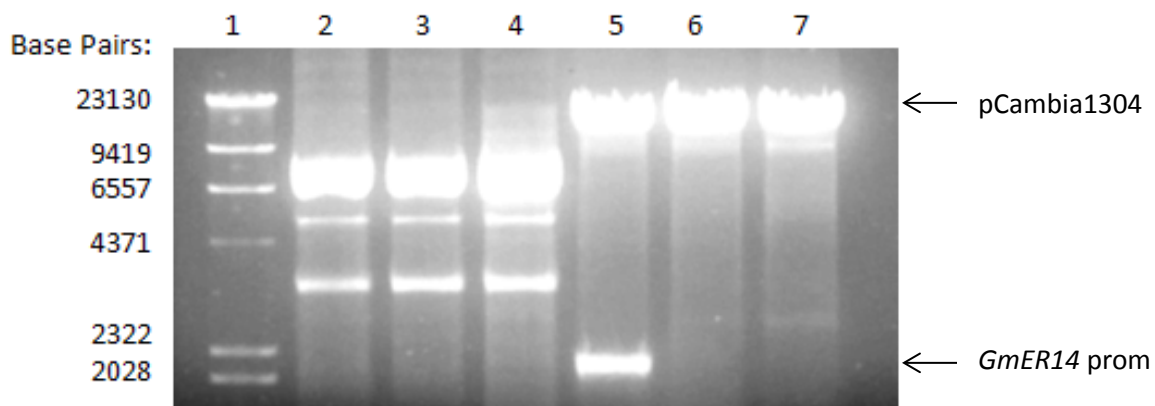


Figure 3: *GmERD14* and pCambia1304 digest with BamHI and NcoI-HF confirms ligation. 1% agarose gel stained with ethidium bromide. Lane 1 contains  $\lambda$  HindIII marker. Lanes 2 through 7 are DNA isolated from separate colonies from *GmERD14* promoter and pCambia1304 ligation that have undergone a double digest to confirm ligation. Expected band sizes are 2160 (*GmERD14* promoter insert) and 11,569 bp (pCambia1304 vector). Presence of both bands in lane 5 indicates ligation occurred in that colony.

(A)

GGCTCGTATGTTGTGGAATTGTGAGCGGATAACAATTCACACAGGAAACAGCTATGACCATGATTACGAATTC  
 GAGCTCGGTACCCGG**GGATCC**ATGTACCAATAAATTAGGTTCCACATCCAACAAATAACAGACTTTACATCCAAC  
 CAAATAAAGAGAAGAAAGAGGGTTAATACAATAAACTAAATAATTAAGAATTTTTACATGATAAAAAAAG  
 CAAAAATGCATATATAATTTAAAAAACAAGGAGATAGAGTATAATTTAGTGATTTAAAAACCGACCATCTATC  
 CATCCTTGAAATCCAAGACATAATGTAGTGTAGCGGATAAAAAACAACGTCCCTCTCTGGCGAGTGCACATAACCC  
 ACAGGCAAAGTGCCAACAGAACTCTCATTCCCGACGCAACTGACTGCCACACACACACACCGACCCTCTGAAGC  
 CGACATTTTGGGGTCCCGCACTTCACCTCCCCACGTTATTTGTCACGTGTCTCGCTCTCCATTGTCACCTTACAG  
 ATCCACCATACCACCGTGTCTCCCTCATCTTTCTACACTTCTCTCTTTTTTCCATCCTCGCACCTCTCAAGCTAT  
 CACTTCACTCGCTACATACTTTTTTTTATTATTCATCAAAATTAATTAATTCTAGAGTTATTTCTCTAGACTATTCTTT  
 TTTTTCAAATATGAATAAAAGTTAAGAAAGTAAATTATCAATAATTTCTTTTTTAATATTTCCATCCTCACATATA  
 ACAGAAATTTGCTTATCTTTAAATTTCTATTATTAATTTATTTTTATAATAATTTTTTATTATTTTCATTTTT  
 ATAGTCAATAAAATAAAATATTAATATAAAACAATAAAATAAACTACTTTTTCTACGAGAATTGGAAAAGATGAC  
 TTATACACATTAATTGATTGATAAAAAATAATTAAGATCTCAAAATGACACACTGTTTTCAATTGCTTTTGTTA  
 TCGAATATTTAAATAGGAAAAAGAAAAAAATGGTTTTACTATTTCTACATATAATTTGAAAAGAATGAATAAA  
 AAATAACGTGATAATTTCATAGTTAAAAATAAAATAAAAAACGTTTTCCAAAATAAACATATTTCTTTTGTGAC  
 AAAGAATATTTGAAAGAAAGTTATTAATAATTGTACCTAATTAGTAAAGCGAATTATTTTCGATAATTGAAATGAT  
 GAGTAAAGTCAATTAGGATTATCAATAATTTTCTTCTACTATTTCCGCCCTAATGTATAAGAGAAATTTGCATA  
 TCTTTTTATAAGATTTTTTTTACTATGATTAATGTGAAATTTTATTGATTATGTTAATAATTAATTTTTTTTTA  
 TAAAAATCTGATTAATTAATCAATTTTCTCAAGTAACAATATATTGGTTAAATGTCTCTCATATCAATATTTTT  
 TTTTTACAAAATATTATTATTTTTTAATAACTTTTGTAGATAATAAAAAATAATGCTATATTAATAAGATAAATT  
 CATTTTCTGCTGGGGGAATTACAAAAAATGACTATCACACGTTCAAAAATTAAGTAAAAAATATTAATTTAACT  
 ACCTATTTAGTTTTTTTTTCATTTTAATTTACAAAATTAACGTTTTATTAATTTTTATTTGTTTTGTTGCAAATA  
 TTTGCTAGGAAATAGAGAAAACAAAAAATTTTCACTATTATTCTGTACAAGTTTTTAAAAATAGAAAAAAA  
 ATATCAACTGTAAATCAATAGTAAAGGAAGAAATGAAAATAAACGAAGTTTCCATTAATTAAGAATATTTTTT  
 TGAAAATAATATAAATTAATAAATTTAATACATTAATTAATTAATCAATTTTAATGATGATTTTTGAAATTAC  
 TAAAAAGGCTTGTATATGGAGTATTACACATGCATGAGGTTGGTATTGAGCAAATTCATAGCGAGTGCATAT  
 GTAGGCGCGTGGAGGAAAGAGAGAATGAACCTCTTTTTCCATAACTTAATTCACACGTCGGTTACCACCTTTT  
 GGGTTTTGGTATTTCTAATCGCGGGAAGTGCGCGTTATGTGAAGTATAAATGGTGCCAGTCTTGACCTTAAA  
 ACCATCCAATCCAATTGAATCTCCAGAGAGAAGAAGAACTTAATCGATCATCACTTCACTTCACTAATACA**CCA**  
**GG**TAGATCTGACTAGTAAAGGAGAAGAACTTT

(B)

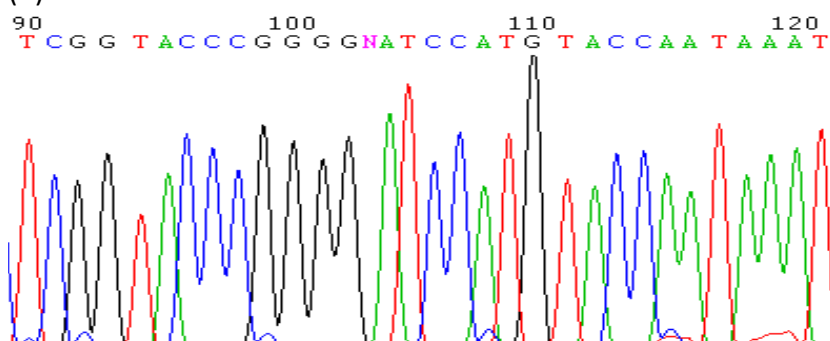


Figure 4: Sequence of *GmERD14* promoter following insertion into pCambia1304.

(A) Green highlight indicates the BamHI restriction site. Red highlight indicates NcoI restriction site. The sequencer lists the underlined A nucleotide as an N (between peak

102 and 104 on the chromatograph), and the following nucleotide as an A. (B) The chromatography shows that the nucleotide following the G at peak 102 should be an A because there is no peak for a nucleotide between the two. Sequencing was performed by the DNA Sequencing Core Facility at IUPUI using GFP reverse, GmERD14 sequencing forward, GmERD14 sequencing reverse1, and GmERD14 sequencing reverse 2 primers.



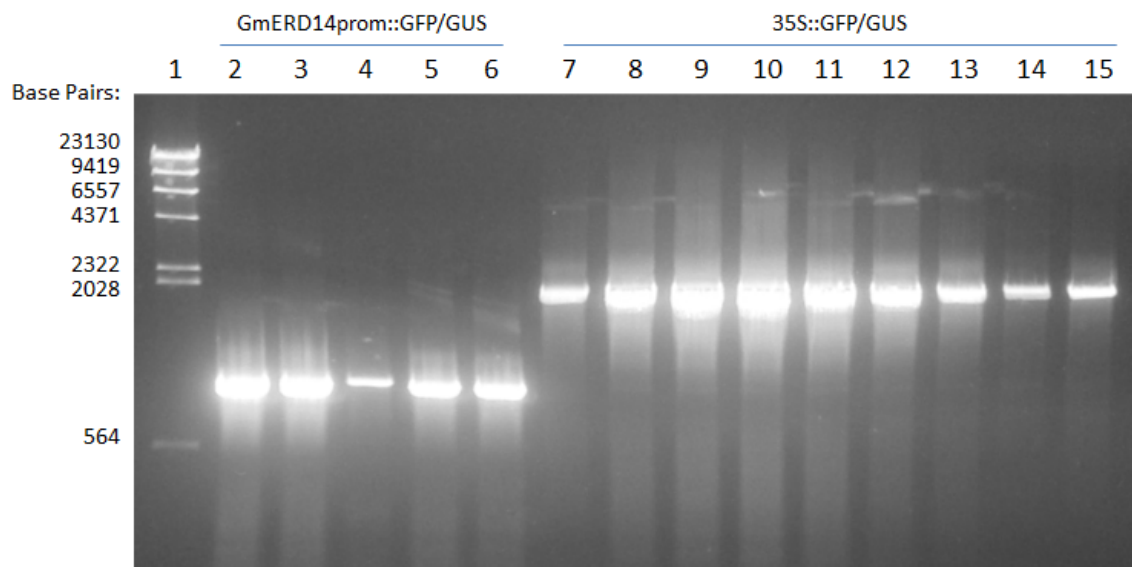


Figure 5: 35S::GFP/GUS and *GmERD14*prom::GFP/GUS stably expressed plant lines contain the insert from transformation.

1% agarose gel. Lane one is  $\lambda$  HindIII marker. Lanes two through six show PCR amplification of DNA isolated from *GmERD14*prom::GFP/GUS lines H, I, J, K, and L in alphabetical order. Lanes seven through 15 contain PCR amplification of DNA isolated from 35S::GFP/GUS lines A through I in alphabetical order. Expected product size of *GmERD14*::GFP/GUS is 965 bp. Expected product size of 35S::GFP/GUS is 2220 bp.

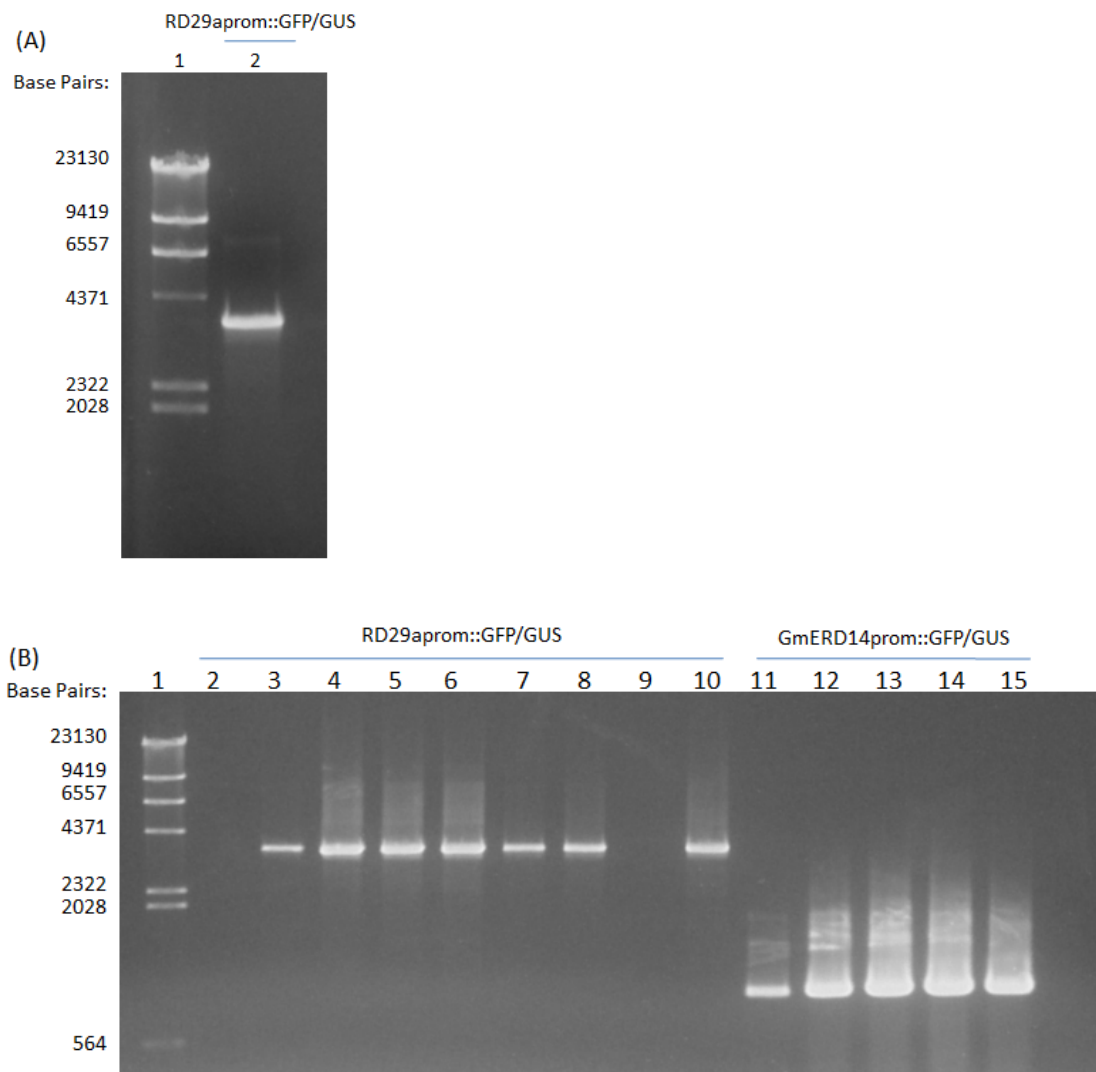


Figure 6: *RD29aprom::GFP/GUS* and *GmERD14prom::GFP/GUS* stably expressed plant lines contain the insert from transformation.

1% agarose gels. (A) Lane one is  $\lambda$  HindIII marker. Lane two is PCR amplification of DNA from *RD29aprom::GFP/GUS* line H. (B) Lane one is  $\lambda$  HindIII marker. Lanes two through 10 show PCR amplification of DNA from *RD29aprom::GFP/GUS* lines B, C, E, F, G, I, K, L, and M in alphabetical order. Lanes 11 through 15 contain PCR amplification of DNA from *GmERD14::GFP/GUS* lines A, C, D, E, and G in alphabetical order. Expected product size of *RD29aprom::GFP/GUS* is 3618 bp. Expected product size of *GmERD14::GFP/GUS* is 965 bp.

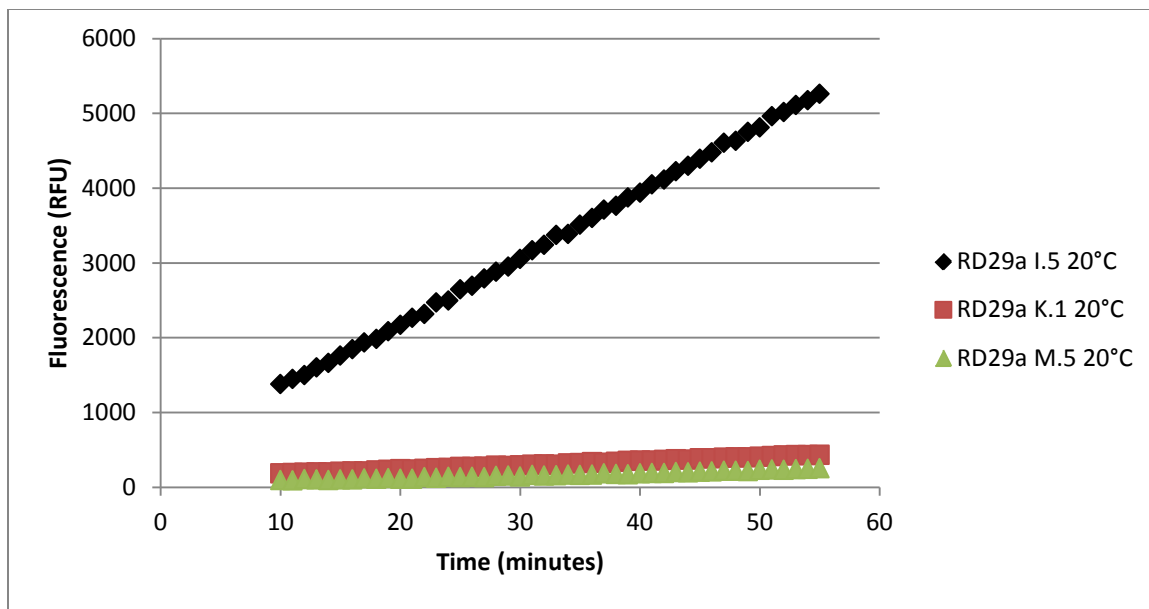


Figure 7: Range of basal level activity in *RD29a*prom::*GFP/GUS* lines.

Representative example of GUS activity of *RD29a*prom::*GFP/GUS* lines measured before cold treatments. Ten  $\mu\text{g}$  of protein were loaded per assay. For line I.5,  $y=87.896x+433.93$  and  $r^2=0.9996$ . For line K.1,  $y=5.769x+121.24$  and  $r^2=0.9967$ . For line M.5,  $y=3.498x+50.558$  and  $r^2=0.9801$ . The basal activities (slope at 20°C) of the other *RD29a*prom::*GFP/GUS* T2 plants were: 193.35 for C.1, 289.41 for C.2, 1.66 for F.1, 5.96 for F.3, 1.9 for H.1, 2.9 for H.5, 192.5 for I.3, 5.1 for K.6, and 1.6 for M.2. Lines B, E, G, and L all had undetectable basal GUS levels and were not used in any other experiments.

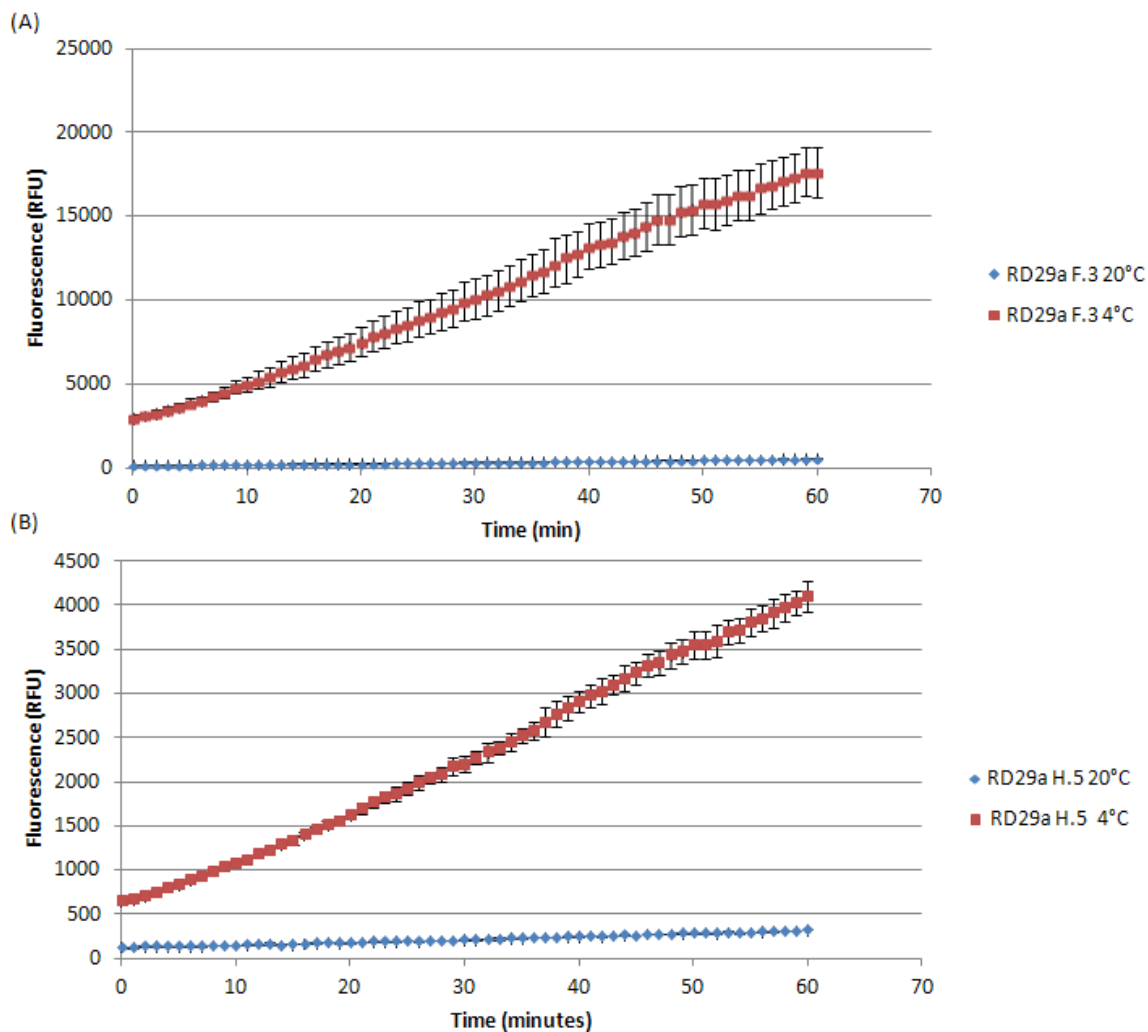


Figure 8: Analysis of GUS activity from *RD29a*prom::GFP/GUS stems. GUS activity of *RD29a*prom::GFP/GUS lines was measured before and after cold treatments. (A) *RD29a* line F.3.  $y=259.23x+2474.8$  at 4°C;  $y=6.7075x+150.63$  at 20°C. (B) *RD29a* line H.5.  $y=59.861x+487.92$  at 4°C;  $y=3.2764x+117.82$  at 20°C. Cold treatment consisted of 24 hours at 4°C. All assays contained 10  $\mu$ g protein from stem extracts. For these experiments,  $n=3$ ; error bars represent standard deviation.

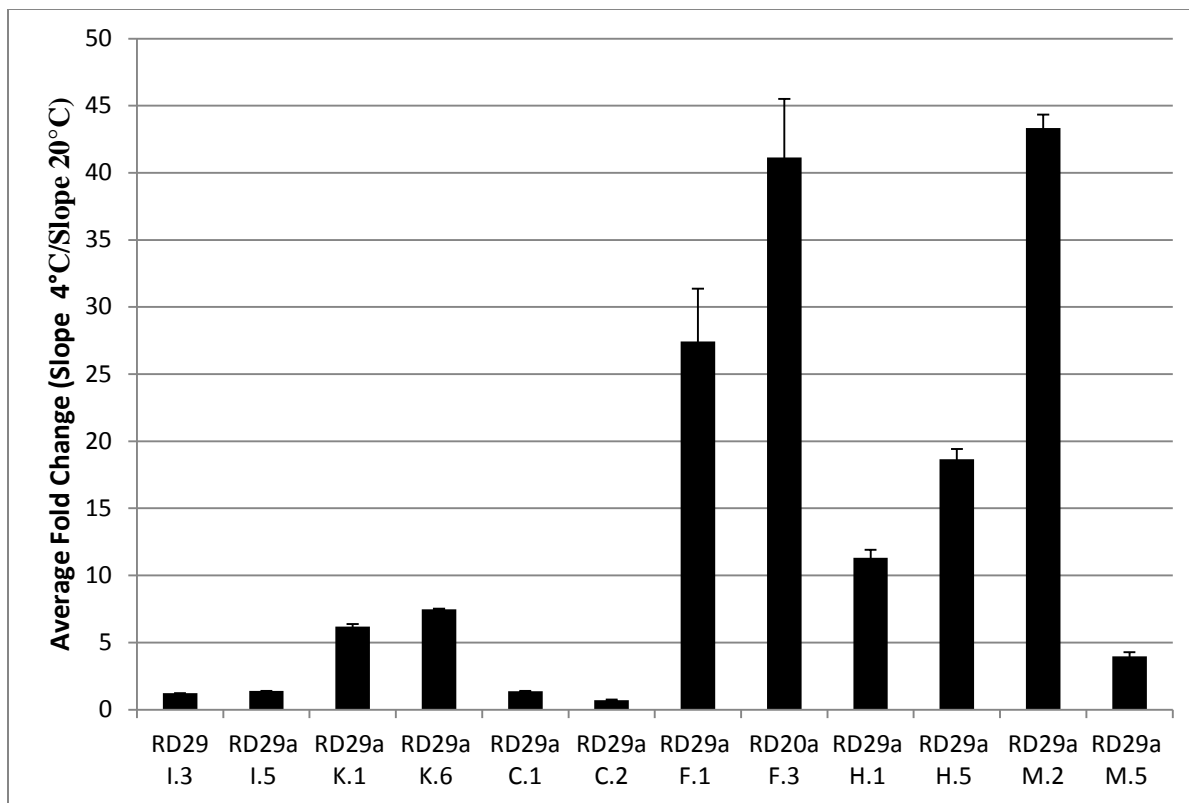


Figure 9: *RD29aprom::GFP/GUS* promoter is cold responsive in T2 stems.

*RD29aprom::GFP/GUS* was stably transformed into wildtype *A. thaliana*. T2 generation stems were collected before and after 24 hour cold treatment at 4°C. Slope of GUS activity before and after cold treatment was measured. Slope = RFU (relative fluorescent unit)/min. Fold change is slope of GUS activity at 4°C/ slope of GUS activity at 20°C. A fold change equal to one indicates no cold induction. A fold change greater than one indicates an increase in GUS activity after cold treatment. For these experiments, n=3. Error bars represent standard deviations.

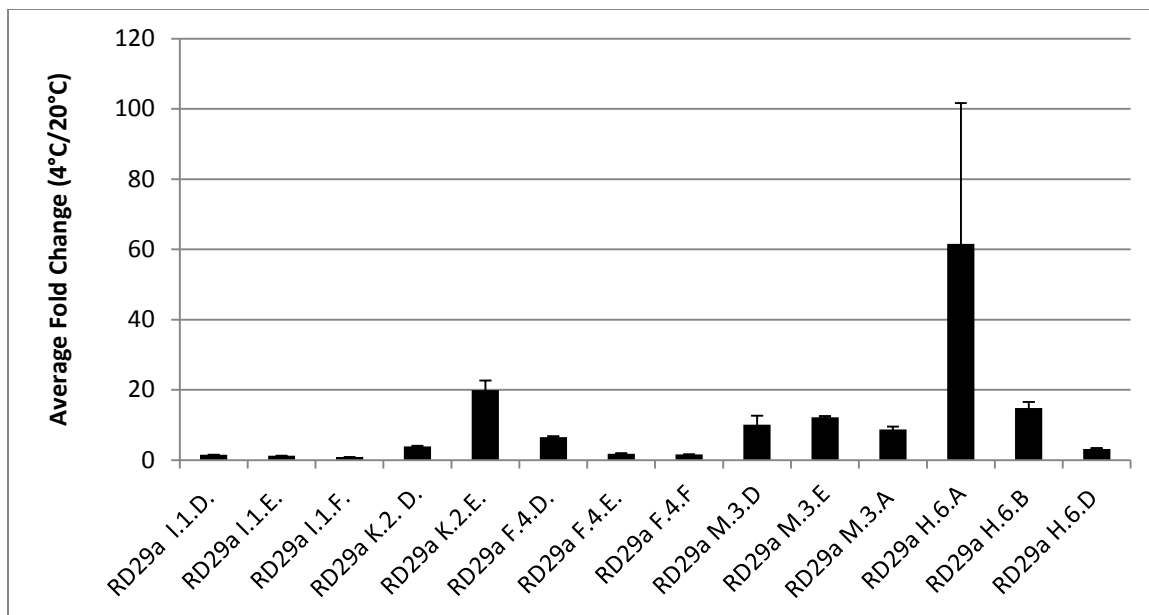


Figure 10: *RD29a*prom::GFP/GUS promoter is cold responsive in T3 leaves.

*RD29a*prom::GFP/GUS was stably transformed into wildtype *A. thaliana*. T3 generation leaves were collected before and after 24 hour cold treatment at 4°C. Slope of GUS activity before and after cold treatment was measured. Slope = RFU (relative fluorescent unit)/min. Fold change is slope of GUS activity at 4°C/ slope of GUS activity at 20°C. A fold change equal to one indicates no cold induction. A fold change greater than one indicates an increase in GUS activity after cold treatment. For these experiments, n=3. Error bars represent standard deviations.

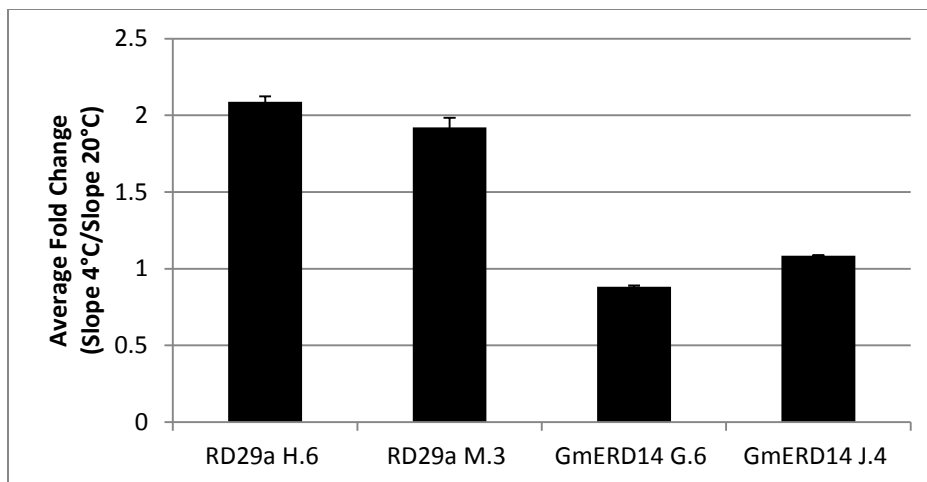


Figure 11: *RD29a*prom::*GFP/GUS* promoter is cold responsive in seedlings, while *GmERD14*prom::*GFP/GUS* reporter does not increase after cold stress. Reporter constructs *RD29a*prom::*GFP/GUS* and *GmERD14*prom::*GFP/GUS* were stably transformed into *Arabidopsis thaliana*. Seedlings then underwent cold treatments consisting of 24 hours at 4°C. Slope of GUS activity in whole seedlings before and after cold treatment was measured. Slope = RFU (relative fluorescent unit)/min. Fold change is slope of GUS activity at 4°C/ slope of GUS activity at 20°C. A fold change equal to one indicates no cold induction. A fold change greater than one indicates an increase in GUS activity after cold treatment. For these experiments, at least twenty seedlings were used per replicate and three replicates were performed. Error bars represent standard deviations.

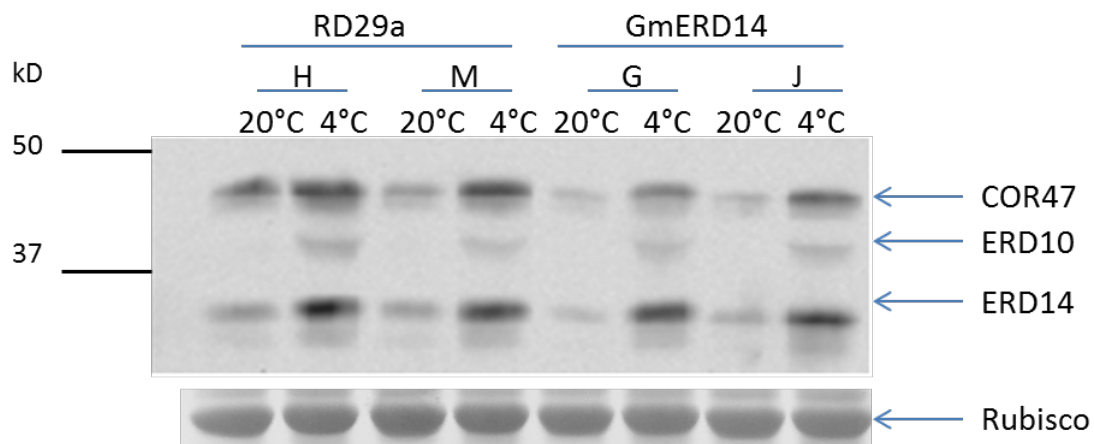


Figure 12: Endogenous AtERD14 protein increases in response to cold stress in *RD29a*prom::GFP/GUS and *GmERD14*prom::GFP/GUS plants.

Reporter constructs *RD29a*prom::GFP/GUS and *GmERD14*prom::GFP/GUS were stably transformed into *Arabidopsis thaliana*. Whole seedlings then underwent cold treatments of 24 hours at 4°C. Western blot used anti-AtERD14 to show endogenous AtERD14 levels before and after cold treatments. Ten µg protein were loaded per lane. Western is representative of three replicates, each replicate containing at least 20 seedlings. Rubisco indicates the SDS-PAGE loading control.



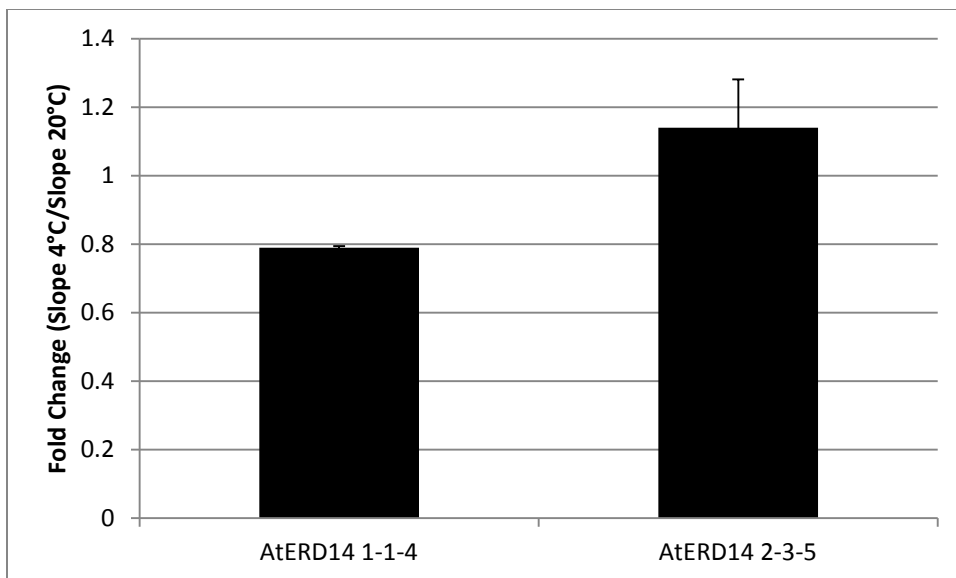


Figure 13: *AtERD14*prom::*GFP/GUS* is not cold responsive in stems

*AtERD14*prom::*GFP/GUS* was stably transformed into wildtype *A. thaliana*. Stems were collected before and after 24 hour cold treatment at 4°C. Slope of GUS activity before and after cold treatment was measured. Slope = RFU (relative fluorescent unit)/min. Fold change is slope of GUS activity at 4°C/ slope of GUS activity at 20°C. A fold change equal to one indicates no cold induction. A fold change greater than one indicates an increase in GUS activity after cold treatment. For these experiments, n=3. Error bars represent standard deviations.

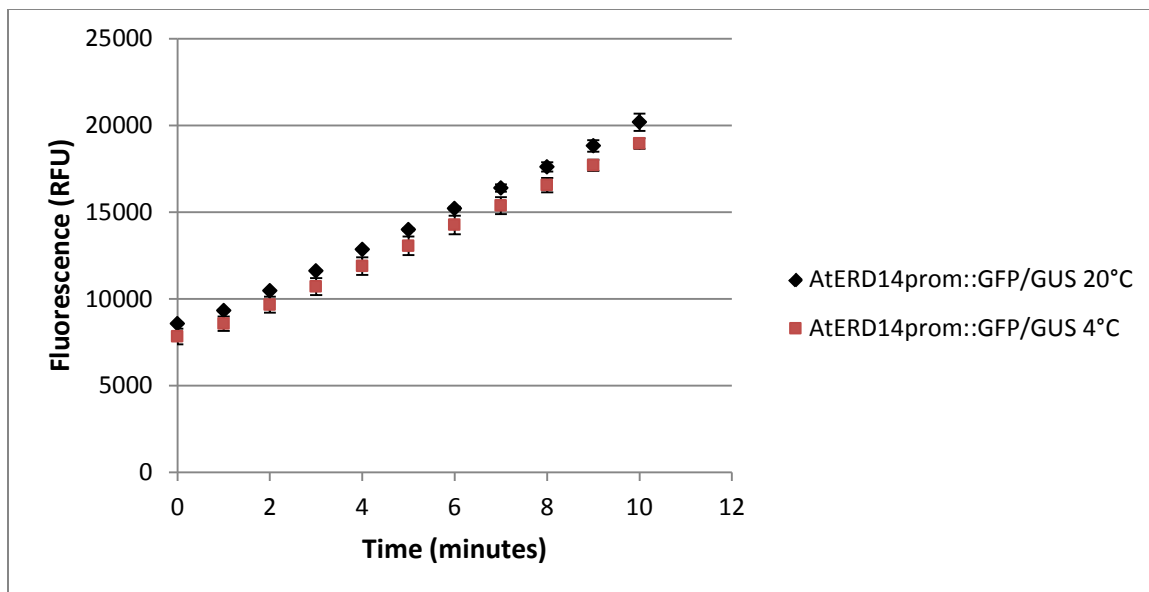


Figure 14: *AtERD14prom::GFP/GUS* is not cold responsive in seedlings

*AtERD14prom::GFP/GUS* was stably transformed into wildtype *A. thaliana*. Whole seedlings were collected before and after 24 hour cold treatment at 4°C. GUS assay fluorescence indicates amount of GUS activity in samples. Ten µg of protein was loaded per assay.  $y=1124.4x+7612.9$  at 4°C;  $y=1160.3x+8271.1$  at 20°C. For these experiments,  $n=3$ . Error bars represent standard deviations.

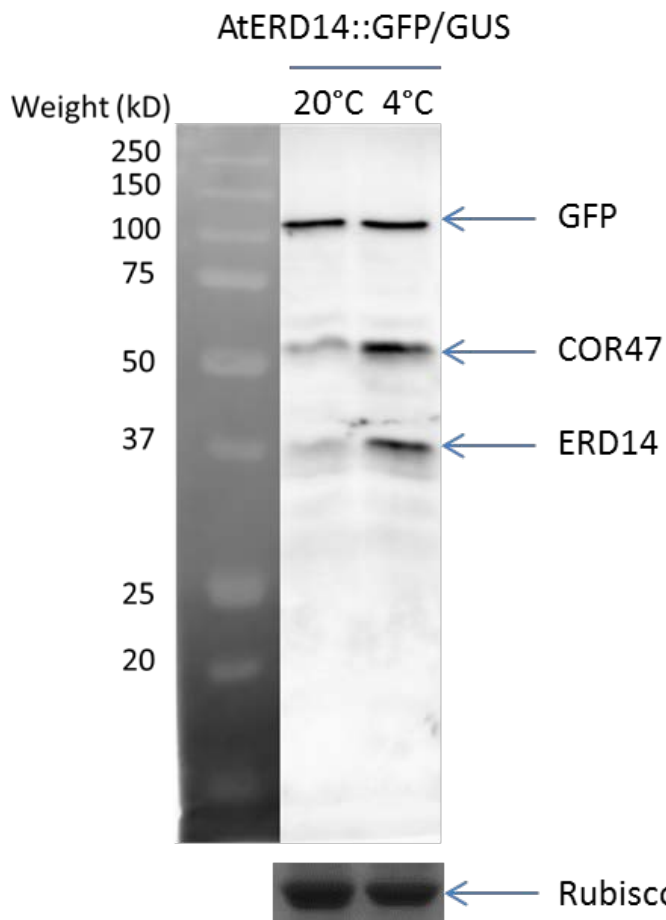


Figure 15: *AtERD14*prom::GFP/GUS endogenous ERD14 increases in response to cold while GFP reporter shows no similar increase.

All cold treatments were for one day at 4°C. Reporter construct *AtERD14*prom::GFP/GUS was stably transformed into wildtype *A. thaliana*. SDS-PAGE was transferred to nitrocellulose membrane. Western blot was performed on two week old seedlings using anti-GFP and anti-ERD14 antibodies. Ten µg protein was loaded per lane. Western is representative of three replications. Rubisco band from SDS-PAGE gel was imaged as loading control. The fold changes (4°C/20°C) for these proteins are: 1.2 for GFP, 2.3 for COR47, and 2.6 for ERD14.

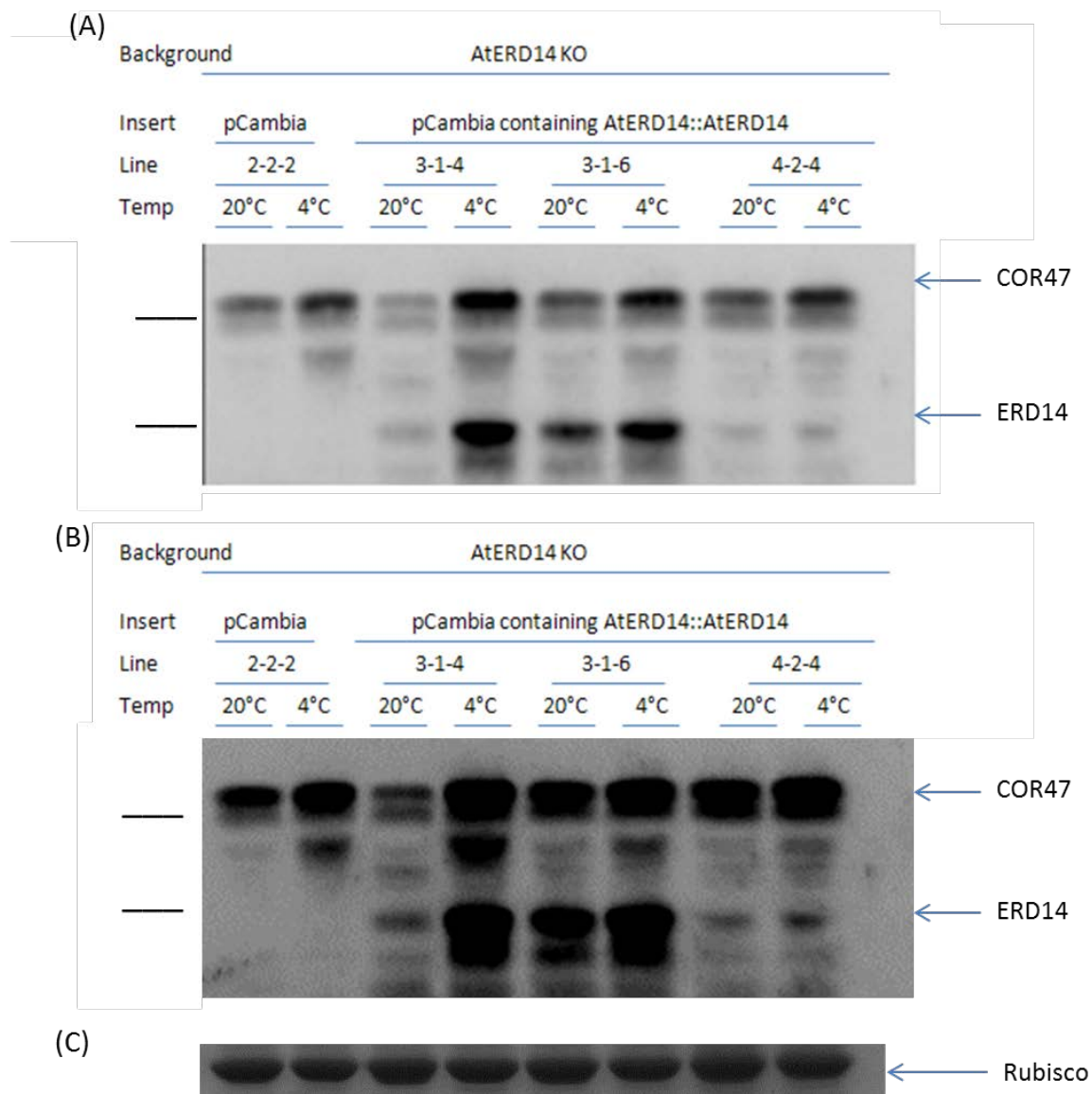


Figure 16: *AtERD14*prom::*AtERD14* expressed in *AtERD14* KO increases in response to cold.

*Arabidopsis thaliana* *AtERD14* knock-out was created and stably transformed with either pCambia 1304 with no insert or containing *AtERD14*prom::*AtERD14*. (A) Western blot was performed on two week old seedlings using anti-ERD14 antibodies. Absence of a band in the pCambia line indicates that ERD14 was successfully knocked out of the lines. Bands in *AtERD14*prom::*AtERD14* lines indicate that ERD14 is present in higher levels in response to cold stress. (B) Longer exposure of blot A to show that line 4-2-4 has increased *AtERD14* protein after cold stress. Each Western is representative of three separate replications. (C) Rubisco band from SDS-PAGE gel was imaged as a loading control.

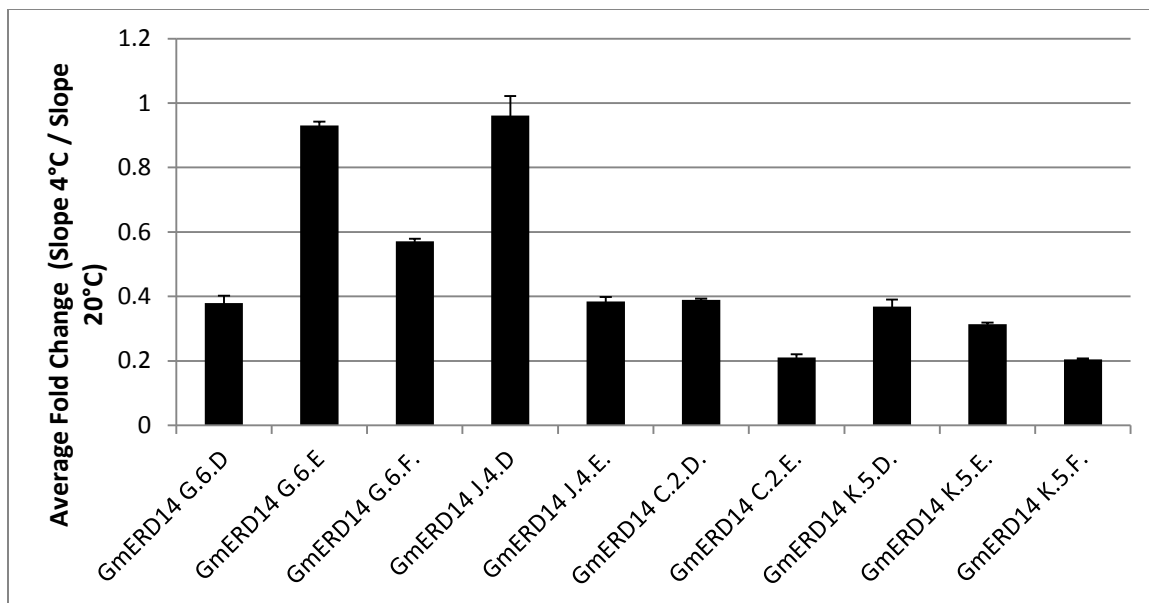


Figure 17: *GmERD14*prom::*GFP/GUS* is not cold responsive in T3 leaves. *GmERD14*prom::*GFP/GUS* was stably transformed into wildtype *A. thaliana*. T3 generation leaves were collected before and after 24 hour cold treatment at 4°C. Slope of GUS activity before and after cold treatment was measured. Slope = RFU (relative fluorescent unit)/min. Fold change is slope of GUS activity at 4°C/ slope of GUS activity at 20°C. A fold change equal to one indicates no cold induction. A fold change greater than one indicates an increase in GUS activity after cold treatment. For these experiments, n=3. Error bars represent standard deviations.

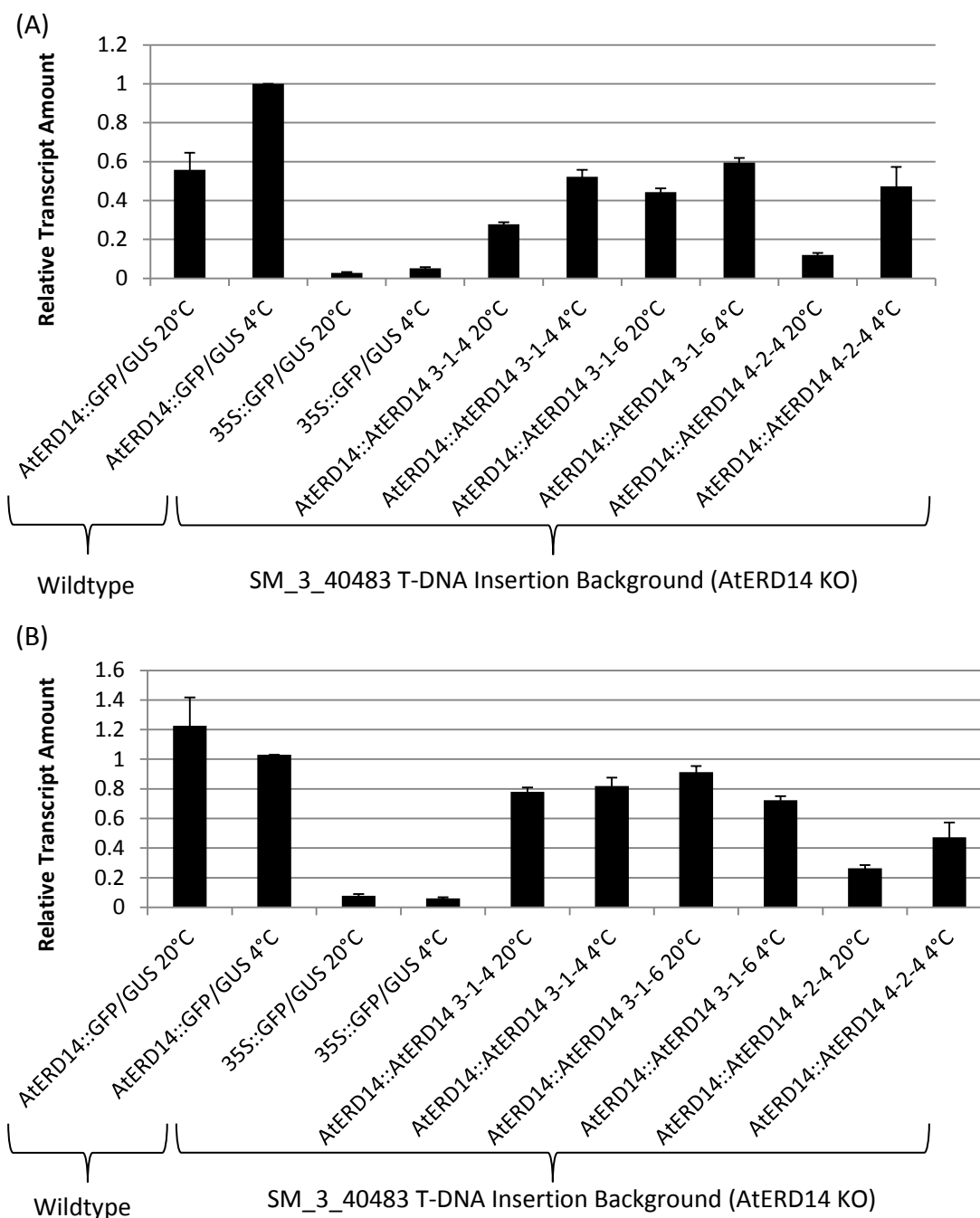


Figure 18: AtERD14 transcript is slightly up-regulated under cold stress when not normalized to AtEF1 $\alpha$ . Stably transformed whole seedlings were collected before and after cold treatments. Cold treatments lasted for 24 hours at 4°C. Wildtype and Sm\_3\_40483 indicate the background the construct was placed into. Sm\_3\_40483 is the T-DNA insert in the coding region of AtERD14 to knock out its activity. (A) The highest amount of transcript was set to 1 and remaining values were quantified relative to that value. (B) AtERD14 values were normalized using AtEF1 $\alpha$  reference gene. For these experiments, n=2. Error bars represent standard deviations.

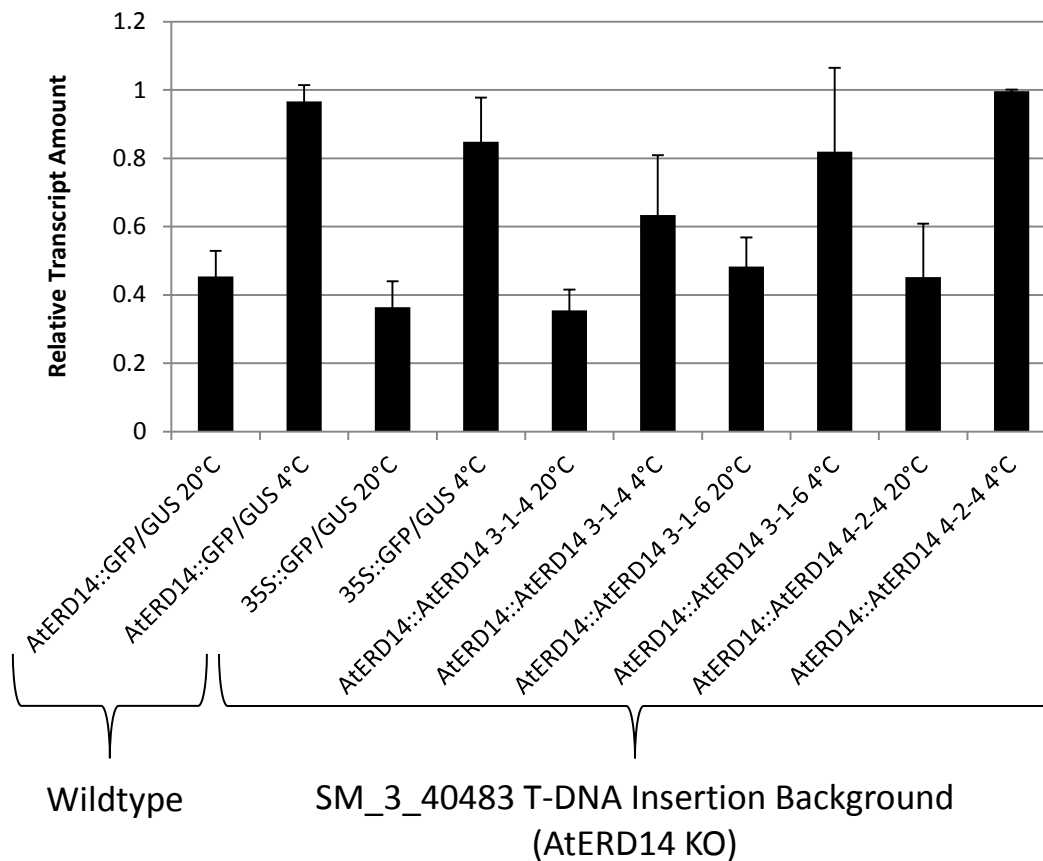


Figure 19: AtEF1 $\alpha$  reference gene transcript is upregulated under cold stress. Stably transformed whole seedlings were collected before and after cold treatments. Cold treatments lasted for 24 hours at 4°C. SM\_3\_40483 is the T-DNA insert in the coding region of *AtERD14* used to knock out its activity. The highest amount of transcript was set to 1 and remaining values were quantified relative to that value. For these experiments, n=2. Error bars represent standard deviations.

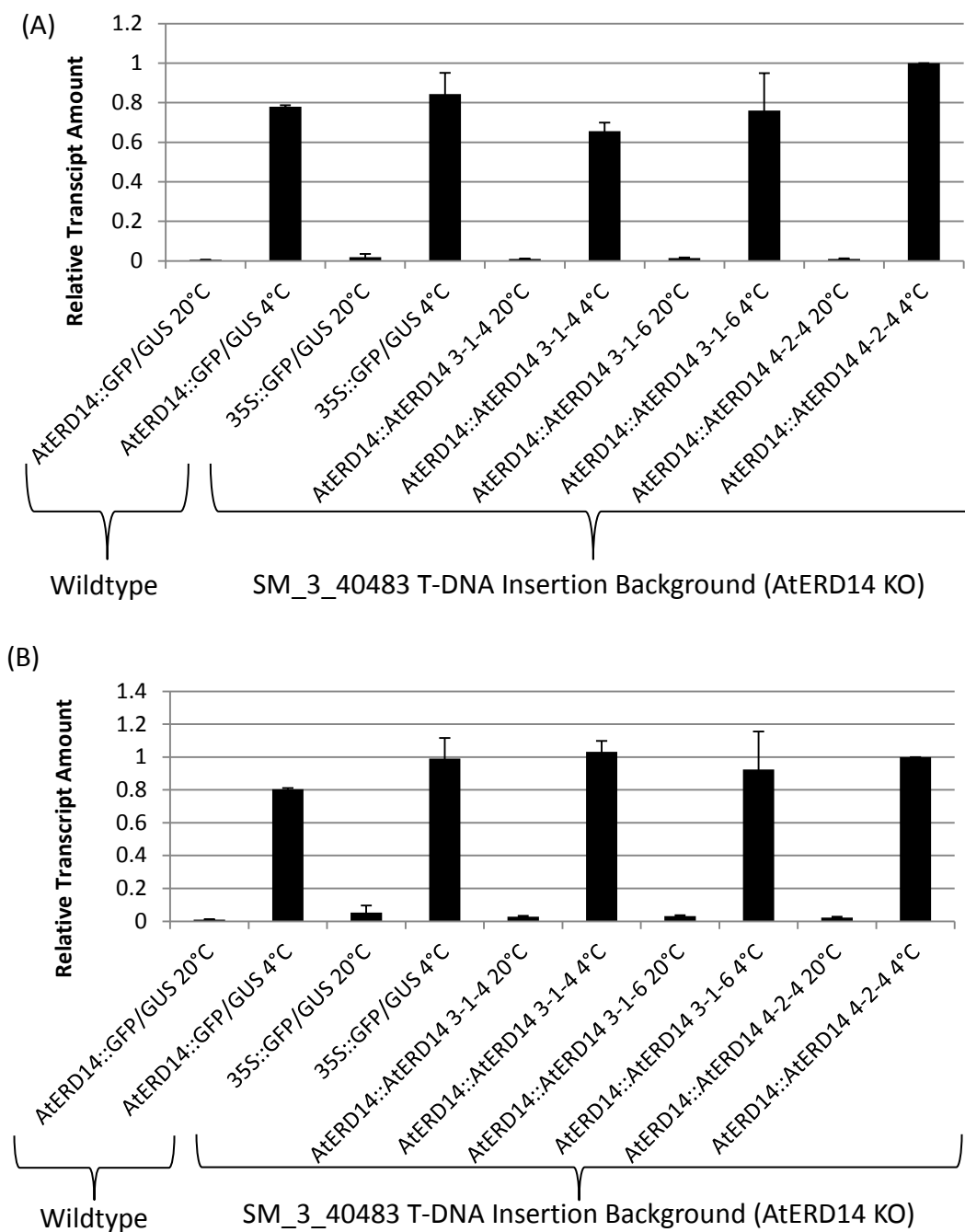
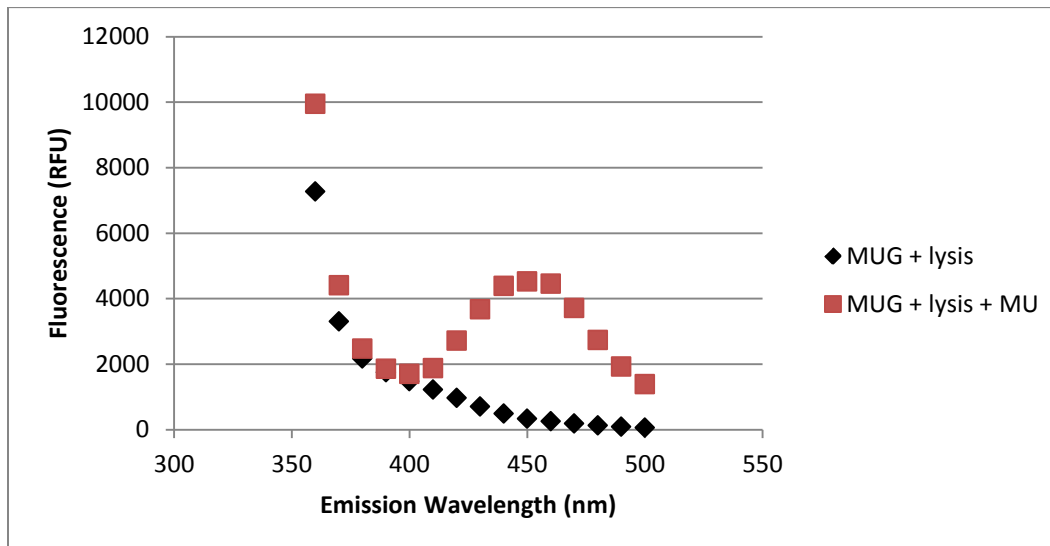


Figure 20: RD29a transcript is strongly up-regulated under cold stress. Stably transformed whole seedlings were collected before and after cold treatments. Cold treatments lasted for 24 hours at 4°C. SM\_3\_40483 is the T-DNA insert in the coding region of *AtERD14* used to knock out its activity. (A) The highest amount of transcript was set to 1 and remaining values were quantified relative to that value. (B) RD29a values were normalized using *AtEF1α* reference gene. For these experiments, n=2. Error bars represent standard deviations.



(A)



(B)

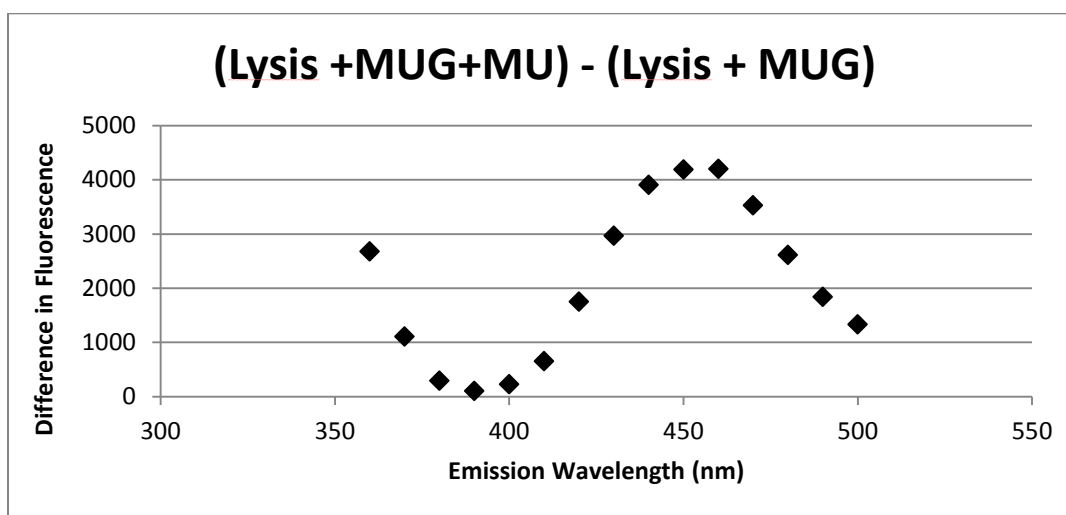
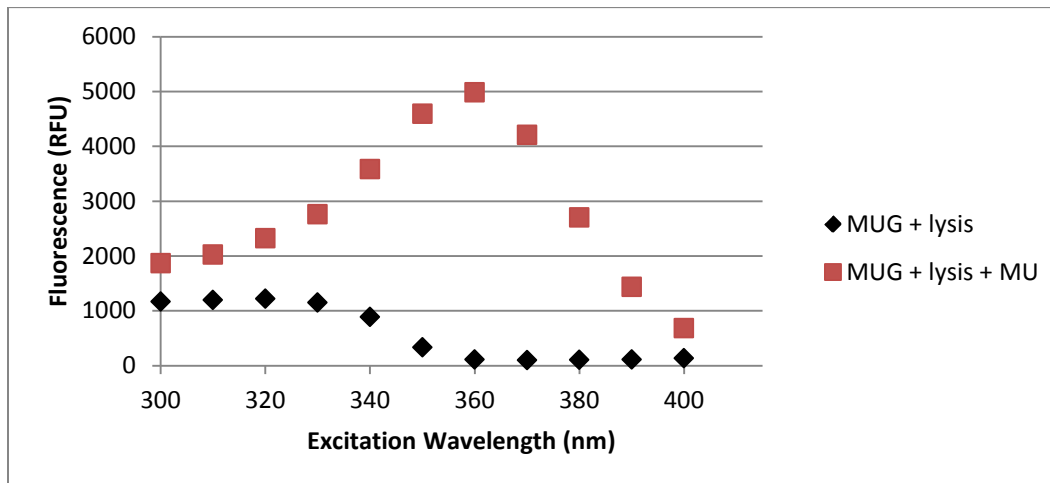


Figure 21: Optimal emission wavelength for detection of MU in the presence of the lysis buffer and MUG is 460nm.

(A) GUS assay was performed using MUG substrate, lysis buffer, and fluorescent MU. Excitation was set at 350nm and the level of fluorescence was measured at emission wavelengths between 350 and 500nm. (B) The value of the fluorescence of the lysis and MUG sample was subtracted from the fluorescence value of the lysis, MUG, and MU sample. Highest point indicates the wavelength with the greatest difference in fluorescence and optimal emission wavelength. These were all performed on a Spectramax Pro 5 fluorometer.

(A)



(B)

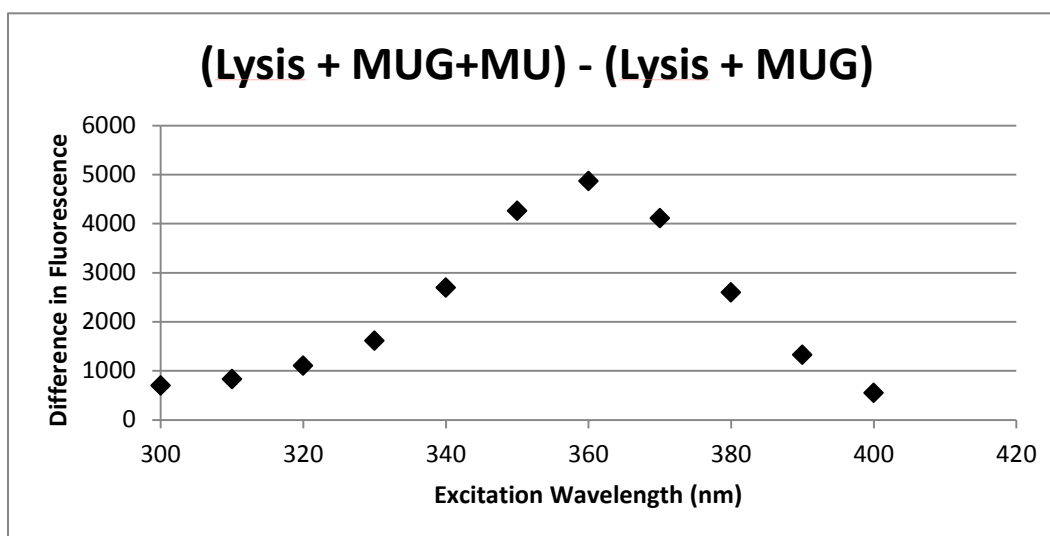


Figure 22: Optimal excitation wavelength for detection of MU in the presence of the lysis buffer and MUG is 360nm.

(A) GUS assay was performed using MUG substrate, lysis buffer, and fluorescent MU. Emission was set at 453nm and the level of fluorescence was measured at emission wavelengths between 300 and 400nm. (B) The value of the fluorescence of the lysis and MUG sample was subtracted from the fluorescence value of the lysis, MUG, and MU sample. Highest point indicates the wavelength with the greatest difference in fluorescence and optimal emission wavelength. These were all performed on a Spectramax Pro 5 fluorometer.

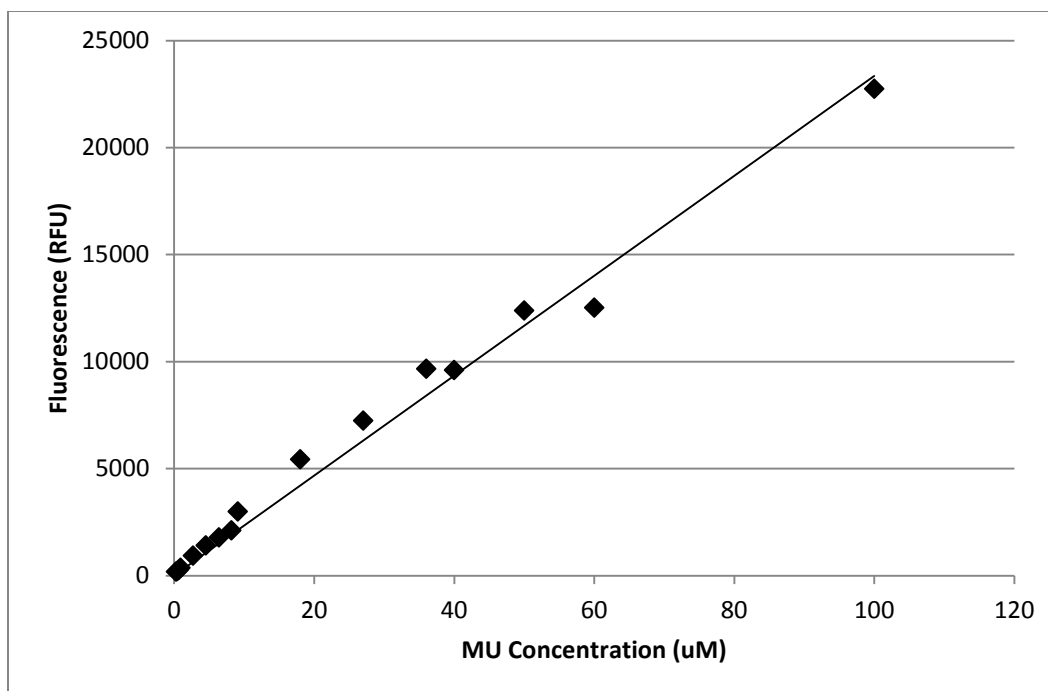


Figure 23: Linearity of GUS Assay, fluorescence as a function of MU concentration. Different concentrations of MU were added to the GUS assay mixture (no GUS). The fluorescence at each concentration was measured and plotted to show the linear range of activity.  $Y=233.55x$ ;  $R^2 = 0.9865$ .

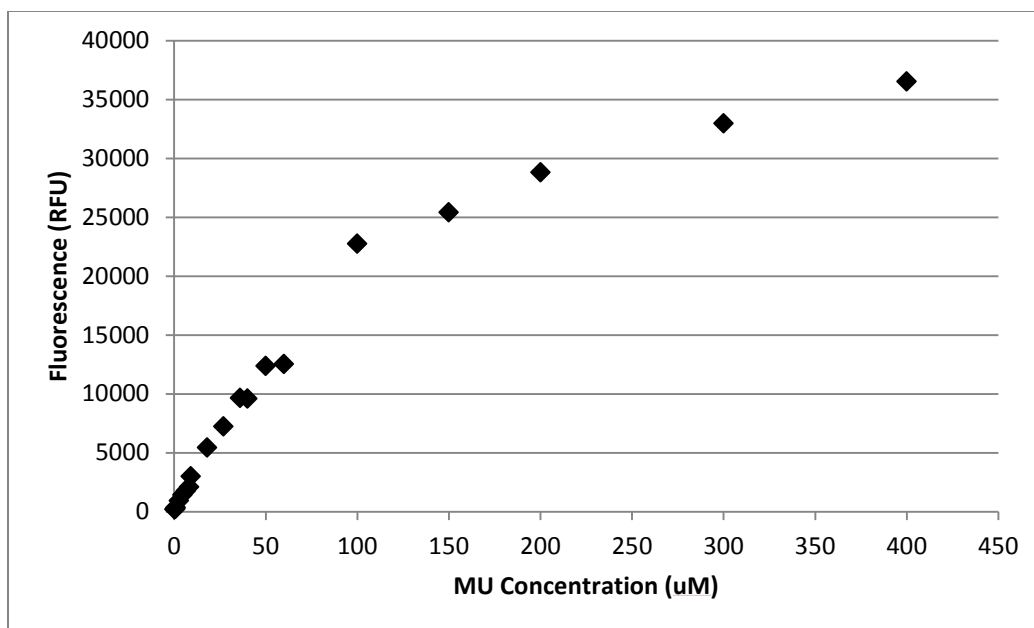


Figure 24: Saturation point of GUS Assay

Different concentrations of MU were added to the GUS assay mixture (no GUS). The fluorescence at each concentration was measured and plotted to show the linear range of activity. Saturation occurs at high concentration.

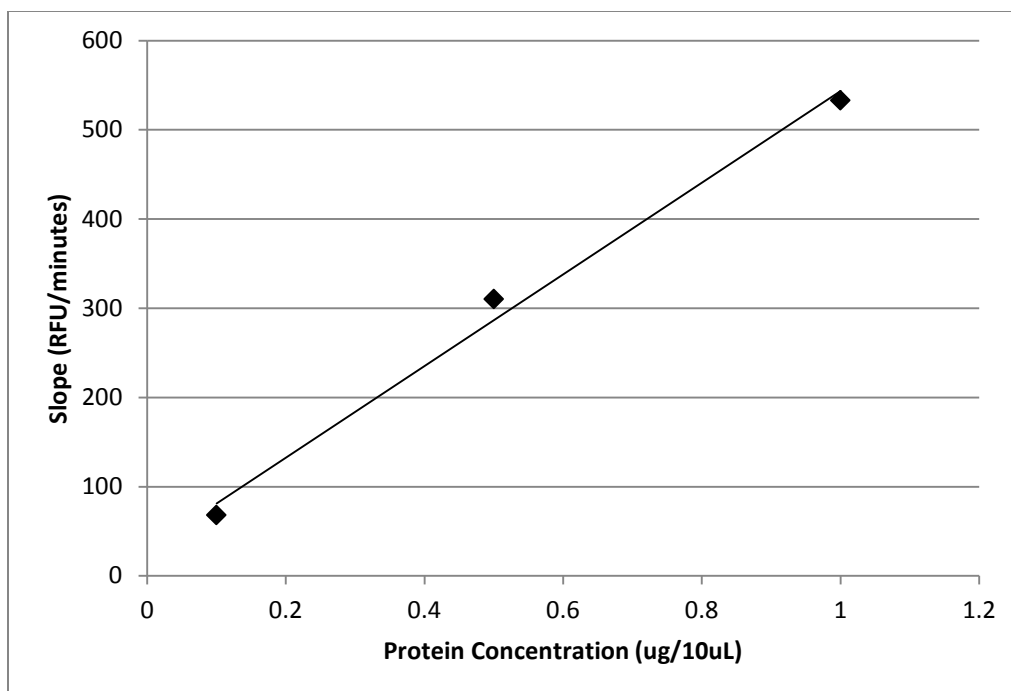


Figure 25: Linearity of GUS Assay as a function of GUS concentration  
*AtERD14prom::GFP/GUS* samples were diluted to show linearity at different concentrations of extracts. Slopes of GUS activity (RFU/minute) for each concentration was calculated and plotted.  $Y=513.48x + 29.935$ .  $R^2=0.9923$ .

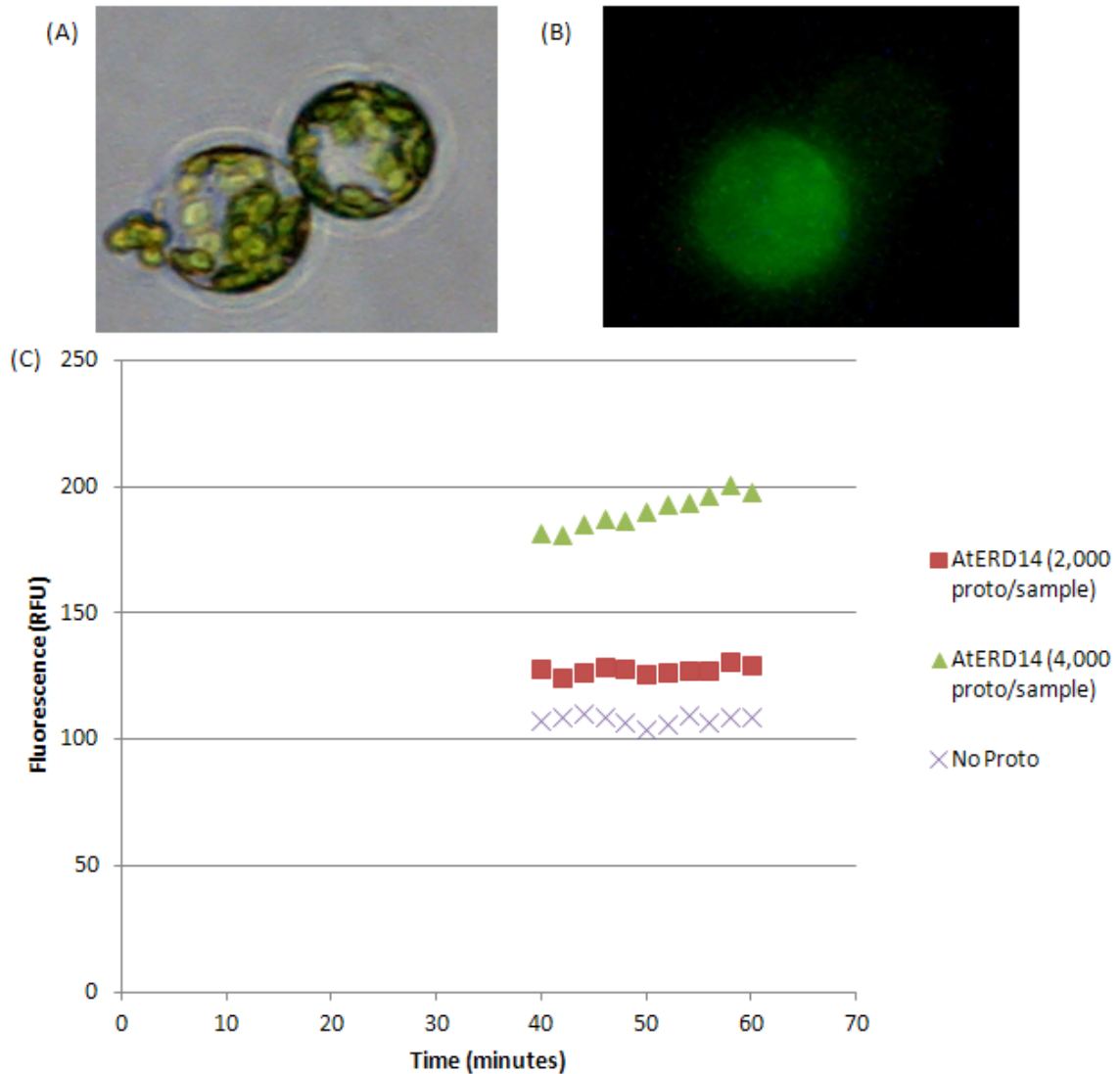


Figure 26: Protoplasts were successfully transiently transformed. Wildtype *A. thaliana* leaves were digested with cellulose and macerozyme. Protoplasts were transformed with *AtERD14*prom::*GUS*/*GFP* using polyethylene glycol (PEG). Transformed protoplasts were visualized after 13 hours by (A) light microscopy or (B) fluorescent microscopy to measure GFP levels. (C) GUS levels were quantitatively measured using a GUS assay.

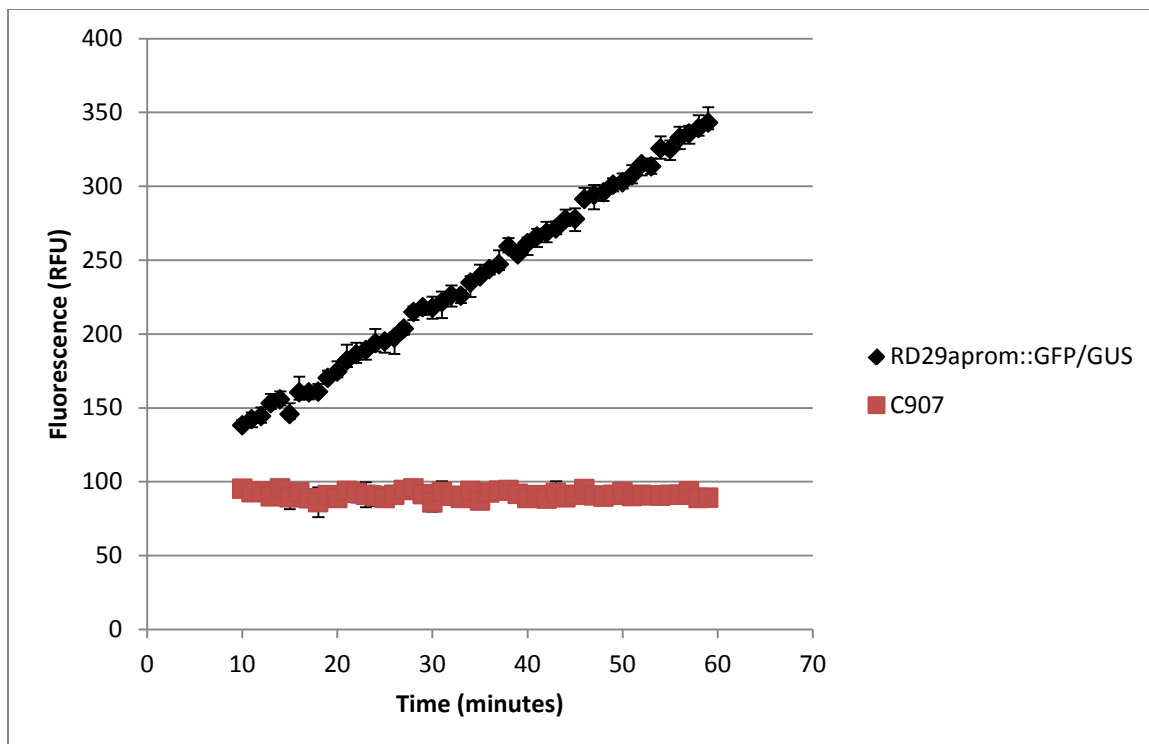


Figure 27: *RD29aprom::GFP/GUS* was successfully transformed into *Arabidopsis thaliana* protoplasts.

C907 indicates wildtype Columbia II *A. thaliana* that were not transformed. For these experiments,  $n=3$ . Error bars represent standard deviations. 100,000 protoplasts were used in each transformation, and 10,000 protoplasts were placed in each GUS assay.

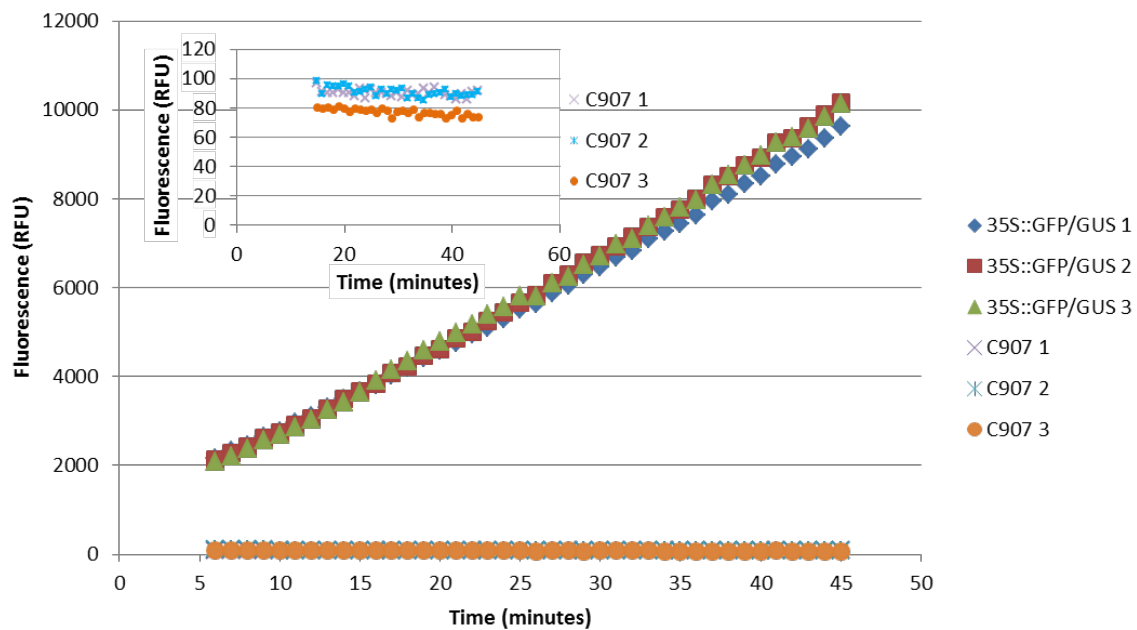


Figure 28: 35S::GFP/GUS is successfully transformed into protoplast cells. Three separate transformation events of the 35S::GFP/GUS vector into wildtype *A. thaliana* (C907) were performed. C907 indicates the wildtype, untransformed protoplasts. Inset graph shows the fluorescence of the untransformed protoplasts on a separate y-axis scale.



## APPENDIX

## APPENDIX

Table A.1: *AtERD14*prom::*GFP/GUS* GUS reporter is not up-regulated after cold stress. Summary of different *AtERD14*prom::*GFP/GUS* cold treatments. Plant lines were stably transformed with *AtERD14*prom::*GFP/GUS*. Tissue samples were collect before and after cold treatments, and basal GUS activity was measured. Fold change indicates the slope of the GUS activity measured at 4°C / the slope of the GUS activity measure at 20°C. N=3.

Line	Sample Type	Length Cold Treatment	Fold Change (Slope 4°C/20°C)	StDEV
<i>AtERD14</i> :: <i>GFP/GUS</i> 1-1-4	Stem	24 hours	0.79	0.004
<i>AtERD14</i> :: <i>GFP/GUS</i> 2-3-5	Stem	24 hours	1.14	0.141
<i>AtERD14</i> :: <i>GFP/GUS</i> 1-1-4	Stem	48 hours	0.89	0.003
<i>AtERD14</i> :: <i>GFP/GUS</i> 1-1-4	Leaves	24 hours	0.58	0.171
<i>AtERD14</i> :: <i>GFP/GUS</i> 1-1-4	Whole Seedlings	24 hours	0.9631	0.302

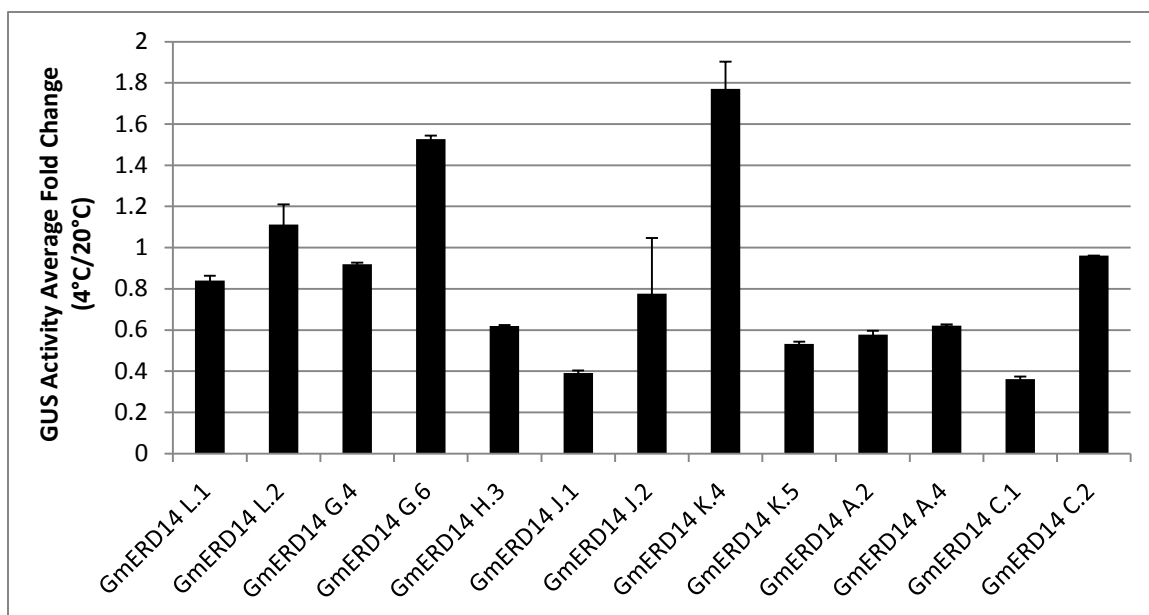


Figure A.1: *GmERD14*prom::*GFP/GUS* promoter is not cold responsive in T2 stems. *GmERD14*prom::*GFP/GUS* was stably transformed into wildtype *A. thaliana*. T2 generation stems were collected before and after 24 hour cold treatment at 4°C. Slope of GUS activity before and after cold treatment was measured. Slope = RFU (relative fluorescent unit)/min. Fold change is slope of GUS activity at 4°C/ slope of GUS activity at 20°C. A fold change equal to one indicates no cold induction. A fold change greater than one indicates an increase in GUS activity after cold treatment. For these experiments, n=3. Error bars represent standard deviations.